



*Supplement of*

## **An aldehyde as a rapid source of secondary aerosol precursors: theoretical and experimental study of hexanal autoxidation**

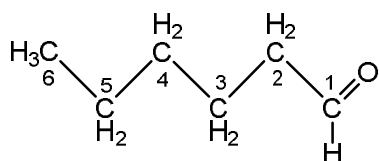
**Shawon Barua et al.**

*Correspondence to:* Shawon Barua ([shawon.barua@tuni.fi](mailto:shawon.barua@tuni.fi)) and Matti Rissanen ([matti.rissanen@tuni.fi](mailto:matti.rissanen@tuni.fi))

The copyright of individual parts of the supplement might differ from the article licence.

## S1: Rate coefficients of H-abstractions predicted by SAR

To place the calculated H-abstraction rate coefficients of hexanal + OH reaction in perspective, we compare them to a structure-activity relationship (SAR) data reported in the literature.<sup>[1,2]</sup> The SAR rate coefficients are calculated by using the formula,  $k_{\text{SAR}} = k_{\text{abs}} \times F(\text{X}) \times F(\text{Y})$  and the resulting values are shown in Supplementary Table S1. Here,  $k_{\text{abs}}$  indicates the rate coefficient associated with the group (-C(=O)H), -CH<sub>2</sub>-, -CH<sub>3</sub>) from which the H atom is being abstracted, where, F(X) and F(Y) are the substituent group factors. For aldehydic H-abstraction on C1, the substituent group factor F(X) corresponds to a -CH<sub>2</sub>- group. Accordingly, for non-aldehydic H-abstraction from the secondary carbon C2, the substituent group factors F(X) and F(Y) correspond to -C(=O)H and -CH<sub>2</sub>- groups respectively.



Supplementary Table S1. Calculated rate coefficients of different H-abstraction reactions in hexanal + OH reaction predicted by SAR.

H-abstraction channels	$k_{\text{abs}}^{\text{a}}$ ( $10^{-12} \text{ cm}^3$ $\text{molecule}^{-1} \text{ s}^{-1}$ )	F(X) <sup>b</sup>	F(Y) <sup>b</sup>	$k_{\text{SAR}}$ ( $10^{-12} \text{ cm}^3$ $\text{molecule}^{-1} \text{ s}^{-1}$ )
C1 (ald H; -C(=O)H)	20.8	1.23 X = -CH <sub>2</sub> -	-	25.58
C2 ( $\alpha$ H; -CH <sub>2</sub> -)	0.77	0.75 X = -C(=O)H	1.23 Y = -CH <sub>2</sub> -	0.71
C3 ( $\beta$ H; -CH <sub>2</sub> -)	0.77	1.23 X = -CH <sub>2</sub> -	1.23 Y = -CH <sub>2</sub> -	1.16
C4 ( $\gamma$ H; -CH <sub>2</sub> -)	0.77	1.23 X = -CH <sub>2</sub> -	1.23 Y = -CH <sub>2</sub> -	1.16
C5 ( $\delta$ H; -CH <sub>2</sub> -)	0.77	1.23 X = -CH <sub>2</sub> -	1.00 Y = -CH <sub>3</sub>	0.95
C6 (prim H; -CH <sub>3</sub> )	0.13	1.23 X = -CH <sub>2</sub> -	-	0.16

<sup>a</sup> values taken from ref. 1 (Jenkin et al. 2018), <sup>b</sup> taken from ref. 2 (Ziemann et al. 2012)

## S2: Bimolecular TST expressions for H-abstraction reactions – a comparison

The rate coefficients ( $k$ ) of the H-abstraction reactions of hexanal by OH, are calculated in three different ways. A simpler approach which is based on the reaction free energy barrier ( $\Delta G^\ddagger$ ) is given in Eq. (1).

$$k = \frac{k_B T}{h^* c} \exp\left(-\frac{G_{\text{TS}} - G_{\text{R}}}{k_B T}\right) \quad (1)$$

The constants,  $k_B$ , and  $h$  are Boltzmann's constant and Planck's constant, respectively. Absolute temperature,  $T$ , is set to 298.15 K.  $c^\circ$  is the total concentration of molecules in

23 standard condition,  $2.46 \times 10^{19}$  molecules  $\text{cm}^{-3}$ .  $G_{TS}$  and  $G_R$  are the Gibbs free energies (at  
 24 298.15 K and 1 atm) of the TS and the reactant, respectively.

25  
 26 The equation that accounts for multiple conformers of TS and hexanal, based on  
 27 multiconformer transition-state theory (MC-TST),<sup>[3]</sup> is shown in Eq. (2).

$$29 \quad k = \sigma \kappa \frac{k_B T}{h^* c^\circ} \frac{\sum_i^{all\ TS\ conf.} \exp\left(-\frac{\Delta E_i}{k_B T}\right) Q_{TS,i}}{Q_{OH} \sum_j^{all\ R\ conf.} \exp\left(-\frac{\Delta E_j}{k_B T}\right) Q_{Hex,j}} \exp\left(-\frac{E_{TS}-E_R}{k_B T}\right) \quad (2)$$

30 where,  $\sigma$  is the symmetry factor,<sup>[4]</sup> and  $\kappa$  is quantum mechanical tunneling.<sup>[5]</sup>  $\Delta E_i$  is the zero-  
 31 point-corrected energy of the  $i^{th}$  TS conformer relative to the lowest-energy transition state  
 32 conformer, and  $Q_{TS,i}$  is the partition function of the  $i^{th}$  transition state conformer. Similarly,  $\Delta E_j$   
 33 and  $Q_{Hex,j}$  are the corresponding values for hexanal conformer  $j$ .  $Q_{OH}$  is the partition function  
 34 of the lowest energy OH conformer.  $E_a = E_{TS}-E_R$  is the zero-point corrected barrier height  
 35 corresponding to the lowest energy TS and reactant conformers. In the case of only lowest-  
 36 energy reactant and TS conformers, Eq. (2) is reduced to Eq. (3) as below. The approach is  
 37 called lowest-conformer TST (LC-TST). The rate coefficients calculated using all the  
 38 approaches are given in Supplementary Table S2.

$$39 \quad k = \sigma \kappa \frac{k_B T}{h^* c^\circ} \frac{Q_{TS}}{Q_{OH} Q_{Hex}} \exp\left(-\frac{E_{TS}-E_R}{k_B T}\right) \quad (3)$$

40  
 41 Supplementary Table S2. Overall reaction and TS energies in kcal/mol of the different OH  
 42 H-abstraction reactions of hexanal along with calculated rate coefficients (in  $\text{cm}^3 \text{molecule}^{-1}$   
 43  $\text{s}^{-1}$ ).

H-abstraction channels	$\Delta G^\ddagger$	$k$ (simple)	$E_a$	$\kappa$	$k$ (LC-TST)	$k$ (MC-TST)
C1 (aldehydic H) <sup>†</sup>	6.75	$2.86 \times 10^{-12}$	-0.58	1.0	$2.84 \times 10^{-12}$	$8.57 \times 10^{-13}$
C2 ( $\alpha$ H)	9.52	$2.67 \times 10^{-14}$	2.0	1.2	$6.36 \times 10^{-14}$	$5.01 \times 10^{-14}$
C3 ( $\beta$ H)	9.18	$4.73 \times 10^{-14}$	1.5	1.05	$9.99 \times 10^{-14}$	$4.50 \times 10^{-14}$
C4 ( $\gamma$ H)	8.79	$9.14 \times 10^{-14}$	0.1	1.47	$2.69 \times 10^{-13}$	$9.22 \times 10^{-14}$
C5 ( $\delta$ H)	10.28	$7.39 \times 10^{-15}$	1.6	1.04	$1.53 \times 10^{-14}$	$5.78 \times 10^{-15}$
C6 (primary H)	10.29	$7.27 \times 10^{-15}$	2.7	1.29	$2.80 \times 10^{-14}$	$1.39 \times 10^{-14}$

44 <sup>†</sup>aldehydic H-abstraction barrier calculated at RHF-RCCSD(T)-F12a/VDZ-F12// MN15/def2-tzvp  
 45 level of theory.  $k_{overall} (simple) = 3.03 \times 10^{-12} \text{cm}^3 \text{molecule}^{-1} \text{s}^{-1}$ ,  $k_{overall} (LC-TST) = 3.32 \times 10^{-12} \text{cm}^3$   
 46  $\text{molecule}^{-1} \text{s}^{-1}$ .

47 Table S2 clearly shows that the overall H-abstraction rate coefficient is dominated by the  
 48 aldehydic H-abstraction channel (C1). Using both approaches, the simple bimolecular TST and  
 49 LC-TST, the overall rate coefficients are similar with values of  $3.03 \times 10^{-12}$  and  $3.32 \times 10^{-12}$   
 50  $\text{cm}^3 \text{molecule}^{-1} \text{s}^{-1}$ , respectively, whereas the overall MC-TST rate coefficient is lower because  
 51 of the aldehydic H-abstraction getting lowered by a factor of around 3. The lower aldehydic H-  
 52 abstraction rate coefficient in the MC-TST approach is due to the contribution of only three TS

53 conformers against 18 hexanal conformers in the partition function term of the Eq. (2). The  
 54 other H-abstraction rate coefficients (C2–C6 channels) show a little increase in both LC-TST  
 55 and MC-TST approaches compared to the simple bimolecular TST approach except a little  
 56 decrease in  $\delta$  H-abstraction (C5 channel) in the MC-TST approach. The  $\gamma$  H-abstraction rate  
 57 coefficient (C4 channel) in the LC-TST approach according to Eq. (3) shows an increase by a  
 58 factor of 2 compared to the simple expression in Eq. (1). The tunneling factor ( $\kappa$ ) in all the H-  
 59 abstraction cases is close to 1, and therefore, it does not seem to have a significant effect in the  
 60 rate coefficients. On the other hand, the symmetry factor ( $\sigma$ ) shows a significant influence in  
 61 the rate coefficients except for the aldehydic H-abstraction. Although the relatively more  
 62 sophisticated bimolecular TST approach (i.e., LC-TST) do not seem to affect the aldehydic H-  
 63 abstraction rate coefficient of hexanal, both LC-TST and MC-TST do have an effect on the  
 64 non-aldehydic H-abstractions as well as the branching ratios.

### 65 **S3: Hindered rotor treatment on H-shift rate coefficients**

66 We perform hindered rotor calculations on Gaussian to identify the hindered rotors, the  
 67 corresponding periodicities and barriers, and the corrected partition functions. In the  
 68 subsequent MESMER simulation, we use the HinderedRotorQM1D method with the Gaussian  
 69 derived periodicities and barriers. The harmonic frequencies corresponding to the hindered  
 70 rotors are removed. Hindered rotor coefficients of all the lowest energy conformers (in an excel  
 71 file) and one MESMER example file are available in the Zenodo data archive  
 72 (<https://doi.org/10.5281/zenodo.8212748>). We also incorporate the corrected partition  
 73 functions in the MC-TST rate coefficients calculated using Eq. (1) of the main manuscript. All  
 74 the rate coefficients, before and after hindered rotor treatment, are presented in Supplementary  
 75 Table S3. While executing the hindered rotor calculations, in one or more conformers, one-to-  
 76 one correspondence between vibrational and internal rotation modes are not achieved.  
 77 Accordingly, hindered rotor treatment is not applied to MESMER rate coefficients for the  
 78 reactions, A61→A61a', D→D51', and D52→D52n', as Gaussian hindered rotor calculations  
 79 failed for their lowest energy TSs. For the reactions, D→D61', and D51→D52n', hindered rotor  
 80 calculations are not achieved for their corresponding products. In the MESMER input file, for  
 81 the reactions with a failed product hindered rotor calculation, we use the product information  
 82 without hindered rotor potential as this is tested to have a minimal effect in the rate coefficient  
 83 (e.g., a factor of 1.1 overestimation tested for A→A61' reaction).

84 Supplementary Table S3. Calculated rate coefficients for H-migration in peroxy radicals before  
 85 and after hindered rotor treatment. The migrating H-atoms are marked in red.

Reactant	Product	Substitution pattern		Span <sup>a</sup>	$k_{MC-TST}$ (s <sup>-1</sup> )	$k_{MC-TST}$ (s <sup>-1</sup> ) hindered rotor	$k_{MESMER}$ (s <sup>-1</sup> )	$k_{MESMER}$ (s <sup>-1</sup> ) hindered rotor
		H-atom	-OO					
A	A61'	-CH <sub>2</sub> -	-C(=O)OO	1,6	$1.69 \times 10^{-1}$	$6.65 \times 10^{-2c}$	2.0	$5.30 \times 10^{-1}$
A	A51'	-CH <sub>2</sub> -	-C(=O)OO	1,5	$3.49 \times 10^{-2}$	$4.48 \times 10^{-2c}$	$1.97 \times 10^{-1}$	$8.70 \times 10^{-2}$
A61	A61a'	-CH <sub>2</sub> -	>CHOO	1,5	$3.90 \times 10^{-3}$	$1.95 \times 10^{-3d}$	$2.05 \times 10^{-2}$	–
A61	A62	-C(=O)OOH	>CHOO	1,8 <sup>†</sup>	$3.72 \times 10^{-6}$	$3.12 \times 10^{-7}$	$1.33 \times 10^{-5}$	$7.32 \times 10^{-6}$

A62	A62a6'	-CH(OOH)-	-C(=O)OO	1,6	2.08	$1.03 \times 10^{-1}$	-	-
A51	A51a6'	-CH <sub>3</sub>	>CHOO	1,6	$2.77 \times 10^{-5}$	$1.47 \times 10^{-5c}$	$2.19 \times 10^{-4}$	$1.32 \times 10^{-4}$
A51	A51a5'	-CH <sub>2</sub> -	>CHOO	1,5	$7.81 \times 10^{-4}$	$3.15 \times 10^{-4c}$	$8.57 \times 10^{-3}$	$6.12 \times 10^{-3}$
D	D61'	-C(=O)H	>CHOO	1,6	$8.63 \times 10^{-1}$	$4.25 \times 10^{-2c}$	4.04	3.58 <sup>b</sup>
D	D51'	-CH <sub>2</sub> -	>CHOO	1,5	$3.91 \times 10^{-2}$	$2.06 \times 10^{-3e}$	$2.15 \times 10^{-1}$	-
A62	A61	-CH(OOH)-	-C(=O)OO	1,8 <sup>†</sup>	$6.92 \times 10^2$	$2.58 \times 10^1$	$7.53 \times 10^2$	$2.89 \times 10^2$
D51	D52	-CH(OOH)-	>CHOO	1,7 <sup>†</sup>	$8.96 \times 10^1$	$7.03 \times 10^1$	$2.41 \times 10^2$	$4.00 \times 10^2$
D52	D52n'	-C(=O)H	>CHOO	1,6	$1.38 \times 10^{-1}$	$1.45 \times 10^{-2f}$	5.15	-
D51	D52n'	-C(=O)H	>CHOO	1,4	$2.67 \times 10^{-2}$	$9.75 \times 10^{-2g}$	$4.43 \times 10^{-2}$	$8.50 \times 10^{-2b}$

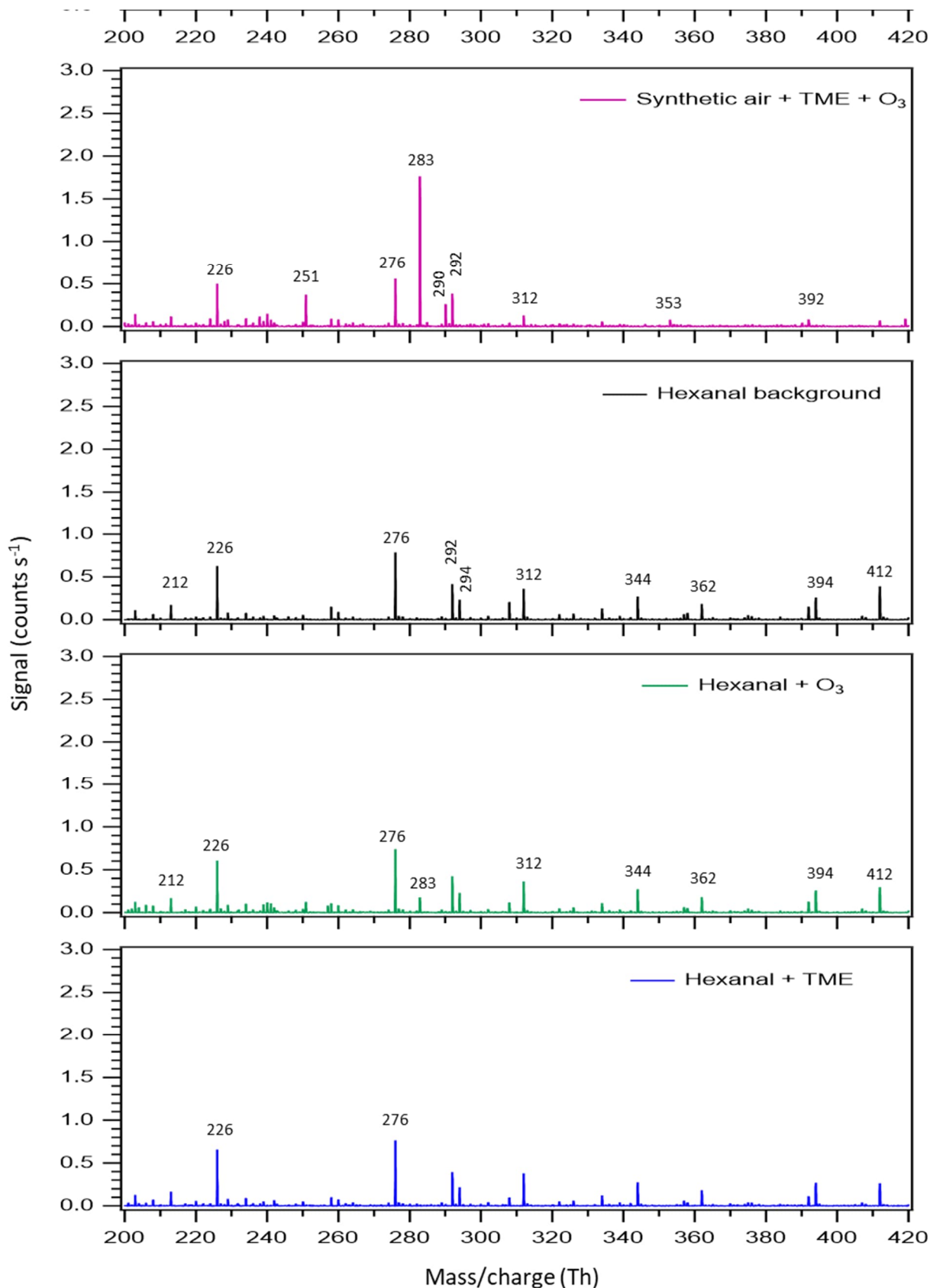
86 <sup>a</sup> H-shift span, <sup>†</sup>H-scrambling reactions, <sup>b</sup> hindered rotor calculation failed for the product  
87 conformer, <sup>c</sup> hindered rotor calculation failed for 1 reactant conformer, <sup>d</sup> hindered rotor  
88 calculations failed for 4 TS conformers, <sup>e</sup> hindered rotor calculations failed for 1 reactant and  
89 1 TS conformer, <sup>f</sup> hindered rotor calculations failed for 5 reactant and 2 TS conformers, <sup>g</sup>  
90 hindered rotor calculation failed for 1 TS conformer.

91 Table S3 shows that the hindered rotor treatment either decreases or increases the MESMER  
92 rate coefficients within a factor of 2 except for the reaction of A→A61' which decreases by a  
93 factor of 3.8. In the MC-TST rate coefficients where hindered rotor calculation failed in one or  
94 more conformers, we use the original partition functions for those conformers instead. The  
95 resultant MC-TST rate coefficients with hindered rotor treatment either decrease or increase  
96 by a factor of around 2 to 3 except for the reaction of D52→A52n' where hindered rotor  
97 calculations failed for five reactant and two TS conformers and decrease the MC-TST rate by  
98 a factor of 9.5.

99

#### 100 **S4: Background spectra in mass spectrometry**

101 In order to ensure that the hexanal + OH oxidation products shown in Figure 6 of the main  
102 manuscript are either distinct or significantly bigger than any background signals, we record  
103 all the possible background spectra separately. Supplementary Figure S1 clearly shows that the  
104 key oxidation products C<sub>6</sub>H<sub>11</sub>O<sub>5-7</sub>, their corresponding closed-shell products C<sub>6</sub>H<sub>10,12</sub>O<sub>5-7</sub> as  
105 well as the accretion products C<sub>12</sub>H<sub>22</sub>O<sub>9-11</sub> are distinct from any background signals originating  
106 from TME + O<sub>3</sub>, hexanal, hexanal + O<sub>3</sub>, and hexanal + TME experiments except the mass of  
107 226 that matches with C<sub>6</sub>H<sub>12</sub>O<sub>5</sub> at unit mass resolution. However, the reported hexanal OH  
108 oxidation spectra in the main manuscript (Figure 6) are all relevant background subtracted  
109 indicating that the product signal C<sub>6</sub>H<sub>12</sub>O<sub>5</sub> (m/z 226) is significant in 3.1 s and 12 s reaction  
110 time experiments.



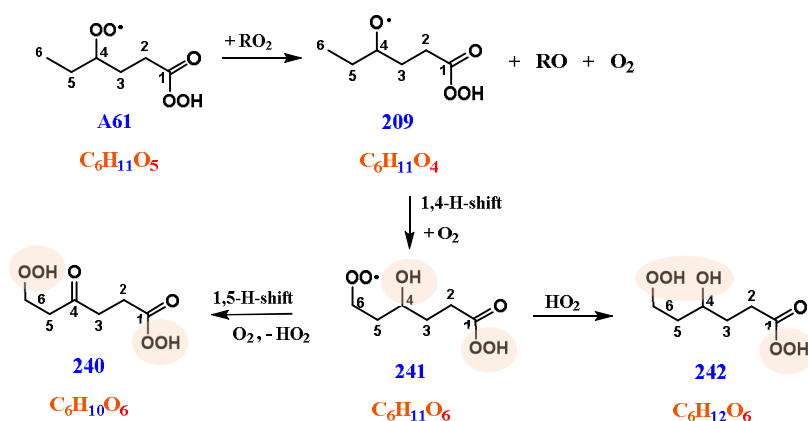
111

112 Figure S1: All background spectra (TME + O<sub>3</sub>, hexanal, hexanal + O<sub>3</sub>, and hexanal + TME)  
 113 recorded during hexanal OH oxidation experiments. The reaction of TME + O<sub>3</sub> is the source  
 114 of the oxidant OH.

115 **S5: Bimolecular reaction products**

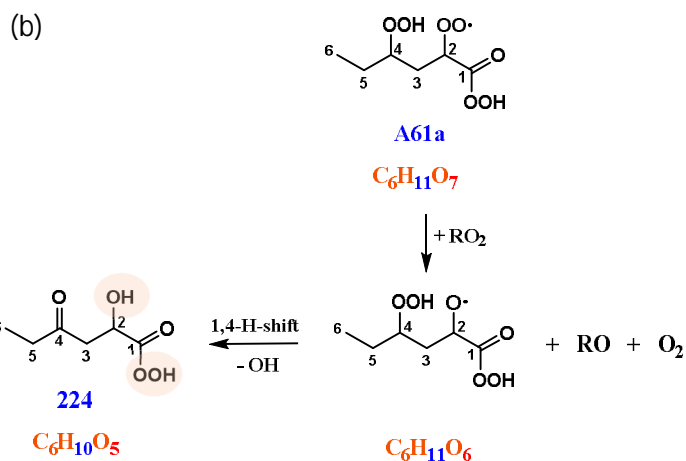
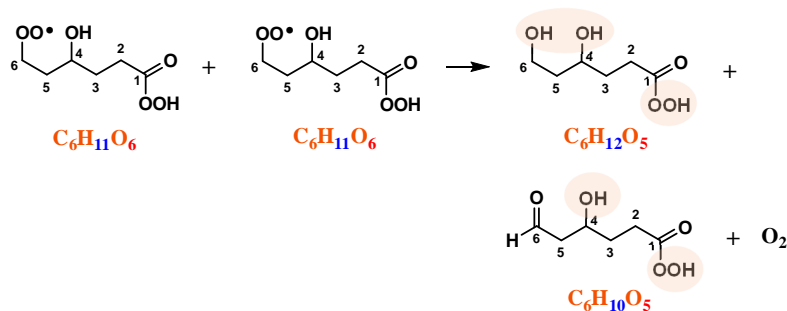
116 This section describes potential reaction mechanisms leading to identified products which  
 117 involve one bimolecular RO<sub>2</sub> + RO<sub>2</sub> reaction step. The labile hydrogen containing groups are  
 118 marked in light-brown shapes. The structures associated with the proposed mechanisms are in  
 119 agreement with the hydrogen to deuterium (H to D) exchange experiments (see Figure 6 in the  
 120 main manuscript).

121 **C<sub>6</sub>H<sub>10-12</sub>O<sub>6</sub>**



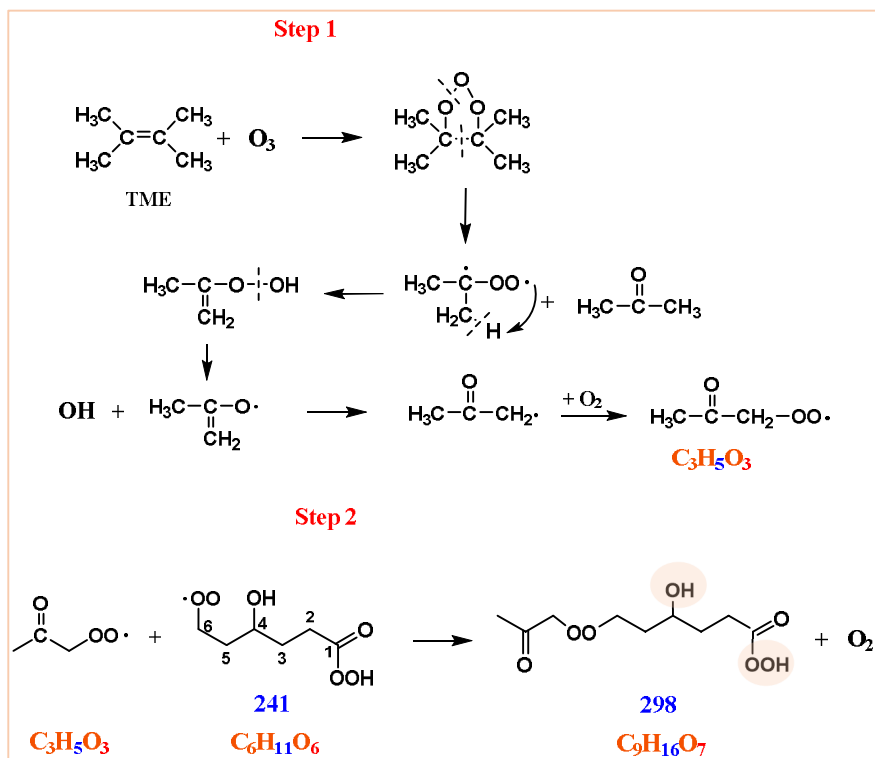
123 Figure S2: Formation of C<sub>6</sub>H<sub>10-12</sub>O<sub>6</sub> products likely involve A61 (C<sub>6</sub>H<sub>11</sub>O<sub>5</sub>) peroxy radical  
 124 undergoing bimolecular reactions with other peroxy radicals in the gas mixture.

125 **C<sub>6</sub>H<sub>10</sub>O<sub>5</sub>**



128 Figure S3: The Russell mechanism producing closed-shell products, an alcohol and a carbonyl  
 129 compound directly from a single RO<sub>2</sub> + RO<sub>2</sub> reaction (a). Formation of C<sub>6</sub>H<sub>10</sub>O<sub>5</sub> product likely  
 130 involves A61a (C<sub>6</sub>H<sub>11</sub>O<sub>7</sub>) peroxy radical undergoing bimolecular reactions with other peroxy  
 131 radicals in the gas mixture (b).

132 **C<sub>9</sub>H<sub>16</sub>O<sub>7</sub>**

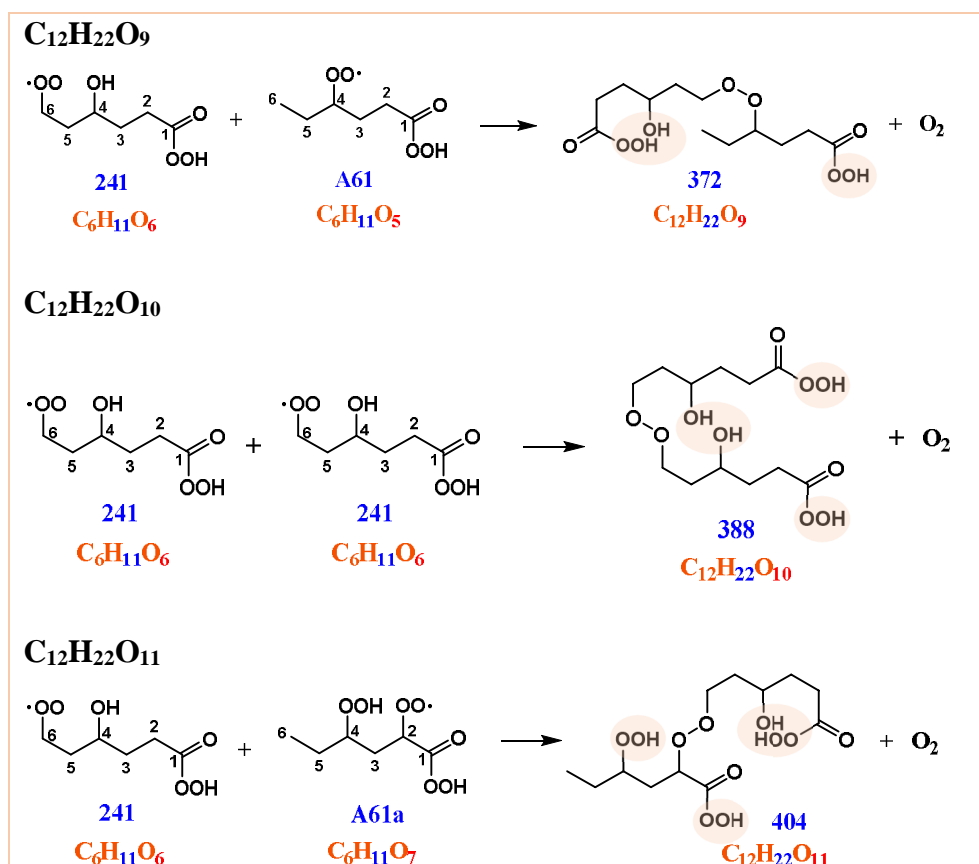


133

134 Figure S4: Production of oxidant OH in tetramethylethylene (TME) ozonolysis. The keto  
 135 peroxy radical C<sub>3</sub>H<sub>5</sub>O<sub>3</sub> is a biproduct and reacts with hexanal derived peroxy radicals yielding  
 136 closed shell products with nine C atoms; a pathway producing C<sub>9</sub>H<sub>16</sub>O<sub>7</sub> peroxide accretion  
 137 product is shown as an example.



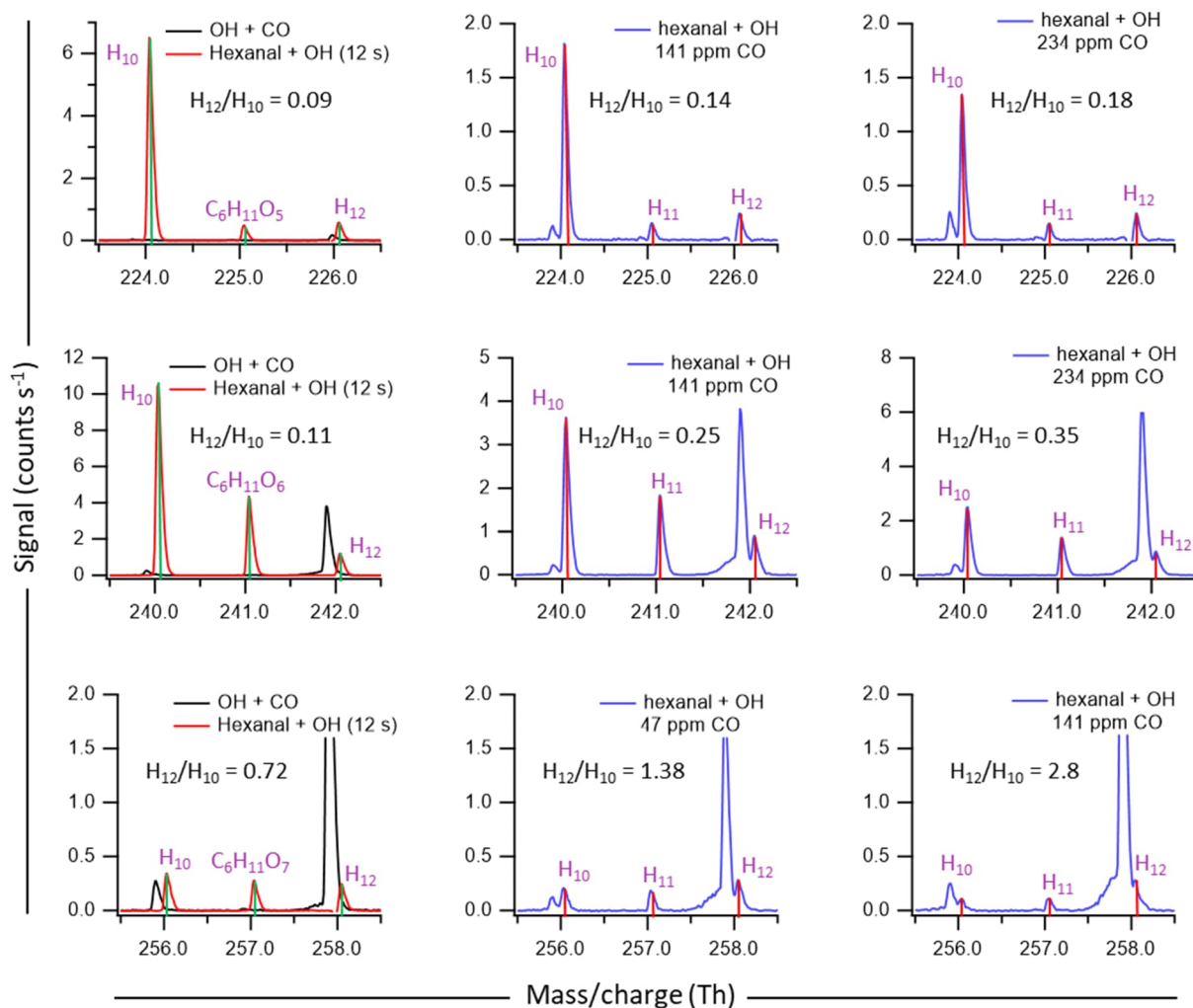
138 **HOM accretion products (C<sub>12</sub>H<sub>22</sub>O<sub>9-11</sub>)**



139 Figure S5: HOM accretion products (C<sub>12</sub>H<sub>22</sub>O<sub>9-11</sub>) are formed by self and cross RO<sub>2</sub> + RO<sub>2</sub>  
 140 reactions.

141 **S6: Hexanal OH oxidation reaction in presence of CO**

142 An additional set of hexanal + OH oxidation experiments are conducted with a variable CO  
 143 concentration ranging from 4–324 ppm. The inclusion of CO in OH-initiated oxidation reaction  
 144 is an additional source of HO<sub>2</sub> (CO + OH  $\xrightarrow{O_2}$  CO<sub>2</sub> + HO<sub>2</sub>) in the reactor. We adopt this technique  
 145 to artificially increase the HO<sub>2</sub> concentration and achieve a control on RO<sub>2</sub> + HO<sub>2</sub> reactions  
 146 leading to the formation of closed-shell C<sub>6</sub>H<sub>12</sub>O<sub>x</sub> (i.e., ROOH) products in our flow reactor.  
 147 The resultant spectra with high-resolution peak fitting are shown in the Supplementary Figure  
 148 S6. It is certain that the inclusion of CO in the reaction mixture introduce more complexity and  
 149 can lead to an overall decrease in the product signals and can produce additional signals.



150

151 Figure S6: Mass spectra showing the key oxidation products ( $C_6H_{10-12}O_{5-7}$ ) with high-  
 152 resolution peak fitting in hexanal OH oxidation reaction in presence of variable concentrations  
 153 of CO. TME ozonolysis ( $TME + O_3$ ) is the source of oxidant OH. The left-most panel of the  
 154 figure presents the spectra under conditions without hexanal ( $CO + OH$ ) and without CO  
 155 (hexanal + OH) added to the flow reactor.

156 While injecting CO, we conduct experiments with and without hexanal to be able to track any  
 157 additional signals originating from OH oxidation where CO cylinder can be a source.  
 158 Apparently, Figure S6 shows that significant background signals originating from CO + OH  
 159 reaction, where TME ozonolysis is the source of OH, are present just left to our product peaks  
 160 of interest (i.e., closed-shell products  $C_6H_{10,12}O_{5-7}$  of hexanal OH oxidation). Despite of the  
 161 presence of these background signals, high-resolution peak fitting of our mass spectrometry  
 162 data allowed us to clearly resolve the closed-shell hexanal OH oxidation products and observe  
 163 the ratio of  $C_6H_{12}O_x$  to  $C_6H_{10}O_x$  (i.e.,  $H_{12}/H_{10}$ ) product peaks in presence of variable CO  
 164 concentrations. We see that with the increase of CO concentration, the  $H_{12}/H_{10}$  ratio is increased  
 165 which supports that the  $RO_2 + HO_2$  reaction can be likely source of closed-shell  $C_6H_{12}O_x$   
 166 products.

## 167 **S7: Kinetic modelling of HOM formation**

168 Kinetic modelling using calculated rate constants is carried out using Kinetiscope Program<sup>[6,7]</sup>  
169 to estimate the time-scale of HOM formation. We include all oxidation initiation channels C1-  
170 C6 and the subsequent steps of the studied C1 and C4 channels in the simulation.

171 In our simulation, we also include bimolecular  $\text{RO}_2 + \text{RO}_2$  and  $\text{RO}_2 + \text{NO}$  reactions with  
172 variable concentrations to see the potential of autoxidation processes in HOM formation under  
173 atmospheric conditions. Initial concentration of hexanal is set to 1 ppb ( $2.46 \times 10^{10}$  molecules  
174  $\text{cm}^{-3}$ ), an average concentration in urban environment.<sup>[8]</sup> In higher aldehydes, the length of the  
175 carbon chain favors HOM formation tendency via autoxidation. Total concentration of  
176 aldehydes (hexanal-decanal) in Monti Cimino forest in Italy was measured to be 8.8 ppb ( $2.16$   
177  $\times 10^{11}$  molecules  $\text{cm}^{-3}$ ).<sup>[9]</sup> We test this concentration as the higher limit of hexanal concentration  
178 to see the influence. A generic concentration of oxidant  $[\text{OH}] = 1.0 \times 10^7$  molecules  $\text{cm}^{-3}$  is used.  
179 A variable concentration of NO (0.01 – 40 ppb, i.e.,  $2.46 \times 10^8$  –  $9.84 \times 10^{11}$  molecules  $\text{cm}^{-3}$ ) is  
180 used to mimic the very clean to very high  $\text{NO}_x$  conditions. A generic value of  $[\text{RO}_2] = 1.0 \times 10^7$   
181 molecules  $\text{cm}^{-3}$  is used for VOC limited condition (high  $\text{NO}_x$ ) and a higher value of  $[\text{RO}_2] = 1.5$   
182  $\times 10^9$  molecules  $\text{cm}^{-3}$  is used for  $\text{NO}_x$  limited condition. For pseudo-unimolecular  $\text{O}_2$  addition  
183 reaction, we use a rate coefficient of  $1 \times 10^7 \text{ s}^{-1}$ . Bimolecular rate coefficients for  $\text{RO}_2 + \text{RO}_2$   
184 and  $\text{RO}_2 + \text{NO}$  reactions are set to the generic values of  $3.2 \times 10^{-11}$  and  $9.0 \times 10^{-12} \text{ cm}^3 \text{ molecules}^{-1}$   
185  $\text{ s}^{-1}$  respectively.<sup>[10,11]</sup>

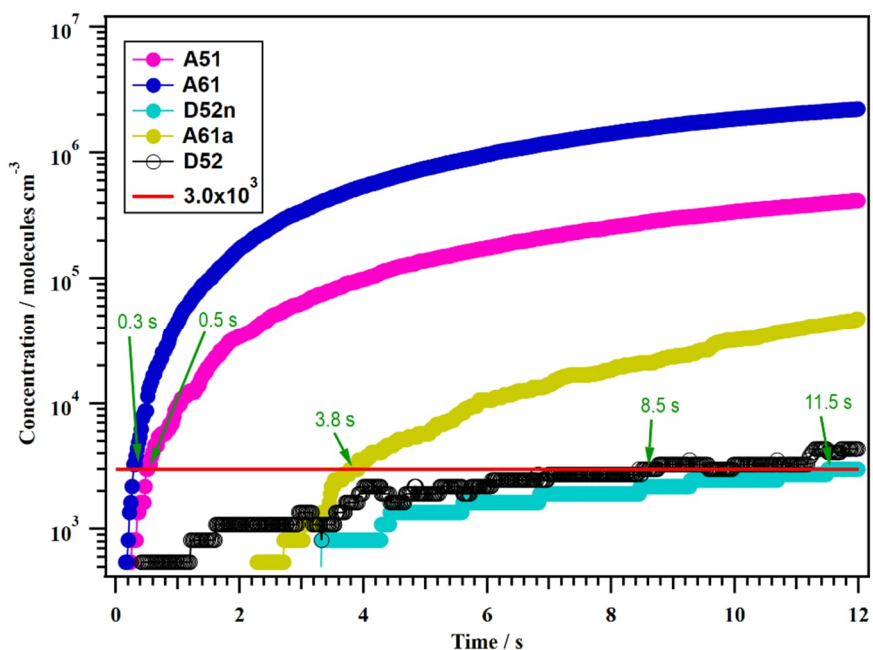
186 One example of the reaction steps is as follows. In this work, we do not study the further  
187 reactions of bimolecular (i.e.,  $\text{RO}_2 + \text{RO}_2$ ,  $\text{RO}_2 + \text{NO}$ , etc.) reaction products. Therefore, in the  
188 simulation, we term the bimolecular products as sinks (e.g., Sink\_a in reaction step 14, Sink\_b  
189 in reaction step 18, and so on).

- 190 1. Hexanal + OH  $\Rightarrow$  A\_pr (aldehydic H-abstraction rate  $k = 2.14 \times 10^{-12} \text{ cm}^3 \text{ molecule}^{-1} \text{ s}^{-1}$ )  
191 1)
- 192 2. A\_pr +  $\text{O}_2 \Rightarrow$  A (pseudo unimolecular rate  $k = 1 \times 10^7 \text{ s}^{-1}$ )
- 193 3. A\_pr  $\Rightarrow$   $\text{C}_5\text{H}_{11}$  + CO ( $\beta$ -scission rate  $k = 2.27 \times 10^3 \text{ s}^{-1}$ )
- 194 4. Hexanal + OH  $\Rightarrow$  B\_pr ( $\alpha$ -H-abstraction rate  $k = 2.66 \times 10^{-14} \text{ cm}^3 \text{ molecule}^{-1} \text{ s}^{-1}$ )
- 195 5. B\_pr +  $\text{O}_2 \Rightarrow$  B
- 196 6. Hexanal + OH  $\Rightarrow$  C\_pr ( $\beta$ -H-abstraction rate  $k = 4.76 \times 10^{-14} \text{ cm}^3 \text{ molecule}^{-1} \text{ s}^{-1}$ )
- 197 7. C\_pr +  $\text{O}_2 \Rightarrow$  C
- 198 8. Hexanal + OH  $\Rightarrow$  D\_pr ( $\gamma$ -H-abstraction rate  $k = 9.16 \times 10^{-14} \text{ cm}^3 \text{ molecule}^{-1} \text{ s}^{-1}$ )
- 199 9. D\_pr +  $\text{O}_2 \Rightarrow$  D
- 200 10. Hexanal + OH  $\Rightarrow$  E\_pr ( $\delta$ -H-abstraction rate  $k = 7.35 \times 10^{-15} \text{ cm}^3 \text{ molecule}^{-1} \text{ s}^{-1}$ )
- 201 11. E\_pr +  $\text{O}_2 \Rightarrow$  E
- 202 12. Hexanal + OH  $\Rightarrow$  F\_pr (primary H-abstraction rate  $k = 7.27 \times 10^{-15} \text{ cm}^3 \text{ molecule}^{-1} \text{ s}^{-1}$ )
- 203 13. F\_pr +  $\text{O}_2 \Rightarrow$  F
- 204 14. A +  $\text{RO}_2 \Rightarrow$  Sink\_a (Alkyl peroxy bimolecular rate  $k = 3.2 \times 10^{-11} \text{ cm}^3 \text{ molecule}^{-1} \text{ s}^{-1}$ )
- 205 15. A + NO  $\Rightarrow$  Sink\_aa (Bimolecular rate  $k = 9.2 \times 10^{-12} \text{ cm}^3 \text{ molecule}^{-1} \text{ s}^{-1}$ )
- 206 16. A  $\Rightarrow$  A61\_pr (1,6-H-shift rate  $k = 1.69 \times 10^{-1} \text{ s}^{-1}$ )
- 207 17. A61\_pr +  $\text{O}_2 \Rightarrow$  A61
- 208 18. A61 +  $\text{RO}_2 \Rightarrow$  Sink\_b
- 209 19. A61 + NO  $\Rightarrow$  Sink\_bb

210 20. A61 => A61a\_pr (1,5-H-shift rate  $k=3.9 \times 10^{-3} \text{ s}^{-1}$ )  
 211 21. A61a\_pr + O<sub>2</sub> => A61a  
 212 22. A61 => A62 (H-scrambling rate  $k=3.27 \times 10^{-6} \text{ s}^{-1}$ )  
 213 23. A62 => A62a6\_pr (1,6-H-shift rate  $k=2.08 \text{ s}^{-1}$ )  
 214 24. A => A51\_pr (1,5-H-shift rate  $k=3.49 \times 10^{-2} \text{ s}^{-1}$ )  
 215 25. A51\_pr + O<sub>2</sub> => A51  
 216 26. A51 + RO<sub>2</sub> => Sink\_c  
 217 27. A51 + NO => Sink\_cc  
 218 28. A51 => A51a5\_pr (1,5-H-shift rate  $k=7.81 \times 10^{-4} \text{ s}^{-1}$ )  
 219 29. A51a5\_pr + O<sub>2</sub> => A51a5  
 220 30. A51 => A51a6\_pr (1,6-H-shift rate  $k=2.77 \times 10^{-5} \text{ s}^{-1}$ )  
 221 31. A51a6\_pr + O<sub>2</sub> => A51a6  
 222 32. D + RO<sub>2</sub> => Sink\_d  
 223 33. D + NO => Sink\_dd  
 224 34. D => D61\_pr (1,6-H-shift rate  $k=8.63 \times 10^{-1} \text{ s}^{-1}$ )  
 225 35. D61\_pr + O<sub>2</sub> => A62  
 226 36. A62 => A61 (H-scrambling rate  $k=6.92 \times 10^2 \text{ s}^{-1}$ )  
 227 37. D => D51\_pr (1,5-H-shift rate  $k=3.91 \times 10^{-2} \text{ s}^{-1}$ )  
 228 38. D51\_pr + O<sub>2</sub> => D51  
 229 39. D51 => D52 (H-scrambling rate  $k=8.96 \times 10^1 \text{ s}^{-1}$ )  
 230 40. D52 + RO<sub>2</sub> => Sink\_e  
 231 41. D52 + NO => Sink\_ee  
 232 42. D52 => D52n\_pr (1,6-H-shift rate  $k=1.38 \times 10^{-1} \text{ s}^{-1}$ )  
 233 43. D52n\_pr + O<sub>2</sub> => D52  
 234 44. D51 => D52n\_pr (1,4-H-shift rate  $k=2.67 \times 10^{-2} \text{ s}^{-1}$ )

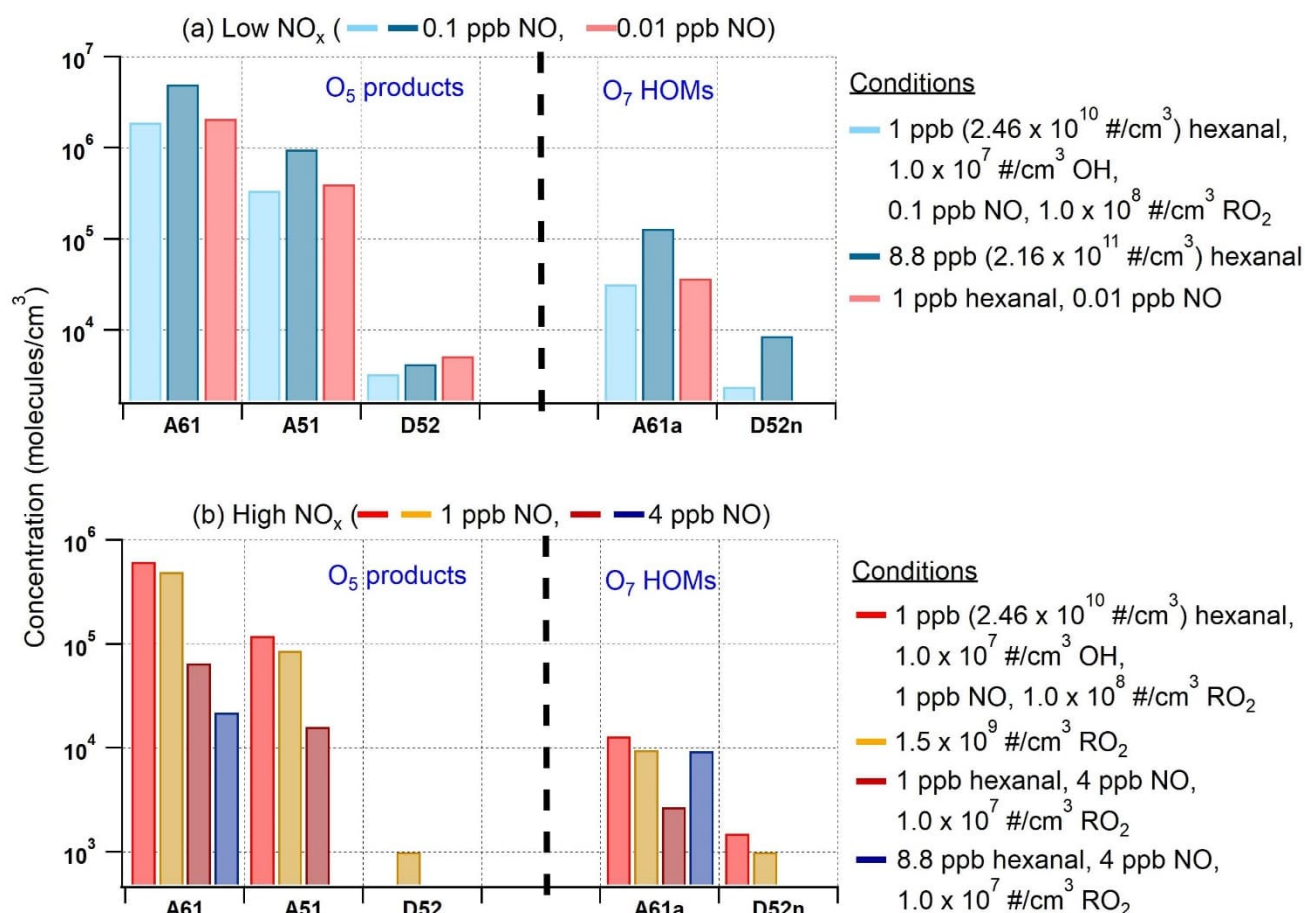
235 The detailed results are given in Supplementary Table S4. For a cleaner environment (1  
 236 ppb= $2.46 \times 10^{10}$  molecules cm<sup>-3</sup> hexanal, 0.1 ppb= $2.46 \times 10^9$  molecules cm<sup>-3</sup> NO, and  $1.0 \times 10^8$   
 237 molecules cm<sup>-3</sup> RO<sub>2</sub>), referring to a product concentration of  $3.0 \times 10^3$  molecules cm<sup>-3</sup>,  
 238 simulation results show that the O<sub>5</sub> intermediates A61 and A51 from C1 channel appear at 0.3  
 239 s and 0.5 s respectively, while D52 from C4 channels appeared at 8.5 s of reaction time (see  
 240 Supplementary Figure S7). The fastest O<sub>7</sub> HOM (A61a at 3.8 s) is associated with the C1  
 241 oxidation channel. On the other hand, the O<sub>7</sub> HOM (D52n) associated with C4 channel appear  
 242 at 11.5 s of reaction time. After 10 s of reaction time, the O<sub>5</sub> intermediates A61 and A51 comes  
 243 with the concentrations of  $1.9 \times 10^6$  and  $3.4 \times 10^5$  molecules cm<sup>-3</sup> respectively while the  
 244 concentration of D52 increases only slightly to  $3.3 \times 10^3$  molecules cm<sup>-3</sup>. Among the O<sub>7</sub> HOM,  
 245 A61a shows the highest concentration ( $3.2 \times 10^4$  molecules cm<sup>-3</sup>) where the concentration of  
 246 D52n is  $2.4 \times 10^3$  molecules cm<sup>-3</sup> at the end of the 10 s simulation reaction time (see light blue  
 247 bars of Supplementary Figure S8a).

248 At this RO<sub>2</sub> and NO level, when we increase the hexanal concentration to 8.8 ppb, the O<sub>5</sub>-  
 249 intermediate and the O<sub>7</sub> HOM concentrations increase by a factor of 3 to 4 with the occurrence  
 250 of A61a HOM concentration of  $4.0 \times 10^3$  molecules cm<sup>-3</sup> as early as 1.7 s reaction time. At 10  
 251 s, the D52 intermediate and D52n HOM concentrations reach at  $4.3 \times 10^3$  and  $8.7 \times 10^3$   
 252 molecules cm<sup>-3</sup> respectively (see blue bars of Supplementary Figure S8a).



253

254 Figure S7: Time profile of hexanal oxidation products showing the appearance of different  
 255 species with five to seven O atoms. Reactant concentrations: hexanal=1ppb ( $2.46 \times 10^{10}$   
 256 molecules  $\text{cm}^{-3}$ ), OH= $1.0 \times 10^7$  molecules  $\text{cm}^{-3}$ , NO=0.1 ppb ( $2.46 \times 10^9$  molecules  $\text{cm}^{-3}$ ), and  
 257 RO<sub>2</sub>= $1.0 \times 10^8$  molecules  $\text{cm}^{-3}$ . The red straight line indicating an arbitrary reference  
 258 concentration of  $3.0 \times 10^3$  molecules  $\text{cm}^{-3}$  intersects the product curves at different reaction  
 259 times (RTs). Among the intermediates with five O atoms, A61 reaches the reference  
 260 concentration very fast at 0.3 s while A51 and D52 reaches at 0.5 and 8.5 s respectively.  
 261 Among the species with seven O atoms, A61a the concentration level at 3.8 s while D52n at 11.5 s.



262

263 Figure S8: Kinetic simulation results showing the distribution of major autoxidation products  
 264 in OH initiated hexanal oxidation reactions with variable precursor concentrations. The  
 265 concentrations presented in the bar plots are extracted after 10 s of simulation time.

266 When the NO concentration is set to a one order of magnitude lower value (0.01 ppb), the  
 267 product concentrations are increased only by a factor of up to 1.6. Increasing the NO  
 268 concentration to 1 ppb, keeping the hexanal concentration at 1 ppb, and RO<sub>2</sub> concentration at  
 269  $1.0 \times 10^8$  molecules cm<sup>-3</sup>, we can still see the appearance of significant O<sub>7</sub> HOM concentrations  
 270 resulting  $1.3 \times 10^4$  and  $1.5 \times 10^3$  molecules cm<sup>-3</sup> for A61a and D52n respectively after 10 s  
 271 reaction time (see red bars of Supplementary Figure S8b). Increasing the RO<sub>2</sub> concentration to  
 272  $1.5 \times 10^9$  molecules cm<sup>-3</sup> at this point, drops the O<sub>7</sub> HOM concentrations by a factor maximum  
 273 1.5 (see orange bars of Supplementary Figure S8b).

274 On the other hand, a NO concentration of 4 ppb stops the production of D52n HOM associated  
 275 with C4 channel regardless of how big the hexanal concentration is while A61a HOM  
 276 associated with C1 channel is still produced after 10 s of reaction time (see Supplementary  
 277 Figure S8b). When we set the NO concentration to the highest (40 ppb), it completely stops the  
 278 formation of any O<sub>5</sub> intermediate and O<sub>7</sub> HOM after 10 s reaction time.

279 Supplementary Table S4: Kinetic modelling results of selected oxidation products  
 280 corresponding to variable reactant concentrations of atmospheric relevance.

Reactant concentrations (#/cm <sup>3</sup> )				Product concentrations (#/cm <sup>3</sup> )				
<i>Hexanal</i>	<i>OH</i>	<i>NO</i>	<i>RO2</i>	O <sub>5</sub> -intermediate			O <sub>7</sub> -HOM	
				<i>A61</i>	<i>A51</i>	<i>D52</i>	<i>A61a</i>	<i>D52n</i>
2.46E+10 (1 ppb)	1.0E+7	2.46E+8 (.01 ppb)	1.0E+7	2.1E+6 <sup>a</sup> (10 s)	4.0E+5 (10 s)	5.2E+3 (10 s)	3.7E+4 (10 s)	1.7E+3 (10 s)
				4.2E+6 (20 s)	8.3E+5 (20 s)	3.2E+3 (20 s)	1.6E+5 (20 s)	1.0E+4 (20 s)
			1.5E+9	1.6E+6 (10 s)	2.8E+5 (10 s)	1.8E+3 (10 s)	2.7E+4 (10 s)	2.4E+3 (10 s)
				2.3E+6 (20 s)	4.5E+5 (20 s)	1.3E+3 (20 s)	1.1E+5 (20 s)	5.2E+3 (20 s)
2.16E+11 (8.8 ppb)	1.0E+7	2.46E+8 (.01 ppb)	1.0E+7	6.2E+6 (10 s)	1.1E+6 (10 s)	8.7E+3 (10 s)	1.2E+5 (10 s)	1.1E+4 (10 s)
				7.1E+6 (20 s)	1.4E+6 (20 s)	0 (20 s)	3.98E+5 (20 s)	1.9E+4 (20 s)
			1.5E+9	4.1E+6 (10 s)	7.9E+5 (10 s)	0 (10 s)	1.2E+5 (10 s)	1.3E+4 (10 s)
				3.1E+6 (20 s)	6.1E+5 (20 s)	0 (20 s)	2.7E+5 (20 s)	1.3E+4 (20 s)
2.46E+10 (1 ppb)	1.0E+7	2.46E+9 (0.1 ppb)	1.0E+8	3.0E+3 <sup>b</sup> (0.3 s)	3.0E+3 (0.5 s)	3.0E+3 (8.5 s)	3.0E+3 (3.8 s)	3.0E+3 (11.5 s)
				1.9E+6 (10 s)	3.4E+5 (10 s)	3.3E+3 (10 s)	3.2E+4 (10 s)	2.4E+3 (10 s)
				3.2E+6 (20 s)	6.1E+5 (20 s)	2.2E+3 (20 s)	1.4E+5 (20 s)	6.8E+3 (20 s)
2.16E+11 (8.8 ppb)	1.0E+7	2.46E+9 (0.1 ppb)	1.0E+8	5.0E+6 (10 s)	9.7E+5 (10 s)	4.3E+3 (10 s)	1.3E+5 (10 s)	8.7E+3 (10 s)
				4.7E+6 (20 s)	9.4E+5 (20 s)	0 (20 s)	3.1E+5 (20 s)	1.3E+4 (20 s)
2.46E+10 (1 ppb)	1.0E+7	2.46E+10 (1 ppb)	1.0E+7	6.3E+5 (10 s)	1.2E+5 (10 s)	4.9E+2 (10 s)	1.2E+4 (10 s)	1.4E+3 (10 s)
				4.6E+5 (20 s)	9.7E+4 (20 s)	1.4E+3 (20 s)	3.5E+4 (20 s)	3.4E+3 (20 s)
			1.0E+8	6.2E+5 (10 s)	1.2E+5 (10 s)	4.9E+2 (10 s)	1.3E+4 (10 s)	1.5E+3 (10 s)
				4.5E+5 (20 s)	9.5E+4 (20 s)	1.9E+3 (20 s)	3.8E+4 (20 s)	3.5E+3 (20 s)
			1.5E+9	4.95E+5 (10 s)	8.7E+4 (10 s)	1.0E+3 (10 s)	9.6E+3 (10 s)	1.0E+3 (10 s)
				3.4E+5 (20 s)	6.7E+4 (20 s)	5.1E+2 (20 s)	3.0E+4 (20 s)	2.0E+3 (20 s)

281 <sup>a</sup> below the product concentrations in the parenthesis are the reaction times. <sup>b</sup> the reaction times colored in red  
 282 indicate how fast the corresponding products appeared, in the simulation.

Reactant concentrations (#/cm <sup>3</sup> )				Product concentrations (#/cm <sup>3</sup> )				
<i>Hexanal</i>	<i>OH</i>	<i>NO</i>	<i>RO2</i>	O <sub>5</sub> -intermediate			O <sub>7</sub> -HOM	
				<i>A61</i>	<i>A51</i>	<i>D52</i>	<i>A61a</i>	<i>D52n</i>
2.16E+11 (8.8 ppb)	1.0E+7	2.46E+10 (1 ppb)	1.0E+7	1.1E+6 <sup>a</sup> (10 s)	2.2E+5 (10 s)	0 (10 s)	5.5E+4 (10 s)	2.4E+3 (10 s)
				1.6E+5 (20 s)	3.8E+4 (20 s)	0 (20 s)	7.5E+4 (20 s)	2.4E+3 (20 s)
			1.0E+8	1.0E+6 (10 s)	2.3E+5 (10 s)	0 (10 s)	3.6E+4 (10 s)	2.4E+3 (10 s)
				1.4E+5 (20 s)	3.4E+4 (20 s)	0 (20 s)	5.5E+4 (20 s)	2.4E+3 (20 s)
			1.5E+9	7.3E+5 (10 s)	1.6E+5 (10 s)	0 (10 s)	4.8E+4 (10 s)	2.4E+3 (10 s)
				7.0E+4 (20 s)	7.3E+3 (20 s)	0 (20 s)	5.3E+4 (20 s)	2.4E+3 (20 s)
2.46E+10 (1 ppb)	1.0E+7	9.84E+10 (4 ppb)	1.0E+7	6.5E+4 (10 s)	1.6E+4 (10 s)	0 (10 s)	2.7E+3 (10 s)	0 (10 s)
				3.4E+4 (20 s)	9.8E+3 (20 s)	1.2E+3 (20 s)	6.1E+3 (20 s)	0 (20 s)
2.16E+11 (8.8 ppb)	1.0E+7	9.84E+10 (4 ppb)	1.0E+7	2.2E+4 (10 s)	0 (10 s)	0 (10 s)	9.4E+3 (10 s)	0 (10 s)
				0 (20 s)	0 (20 s)	0 (20 s)	9.4E+3 (20 s)	0 (20 s)
2.46E+10 (1 ppb)	1.0E+7	9.84E+11 (40 ppb)	1.0E+7	0 (10 s)	0 (10 s)	0 (10 s)	0 (10 s)	0 (10 s)
				0 (20 s)	0 (20 s)	0 (20 s)	0 (20 s)	0 (20 s)
2.16E+11 (8.8 ppb)	1.0E+7	9.84E+11 (40 ppb)	1.0E+7	0 (10 s)	0 (10 s)	0 (10 s)	0 (10 s)	0 (10 s)
				0 (20 s)	0 (20 s)	0 (20 s)	0 (20 s)	0 (20 s)

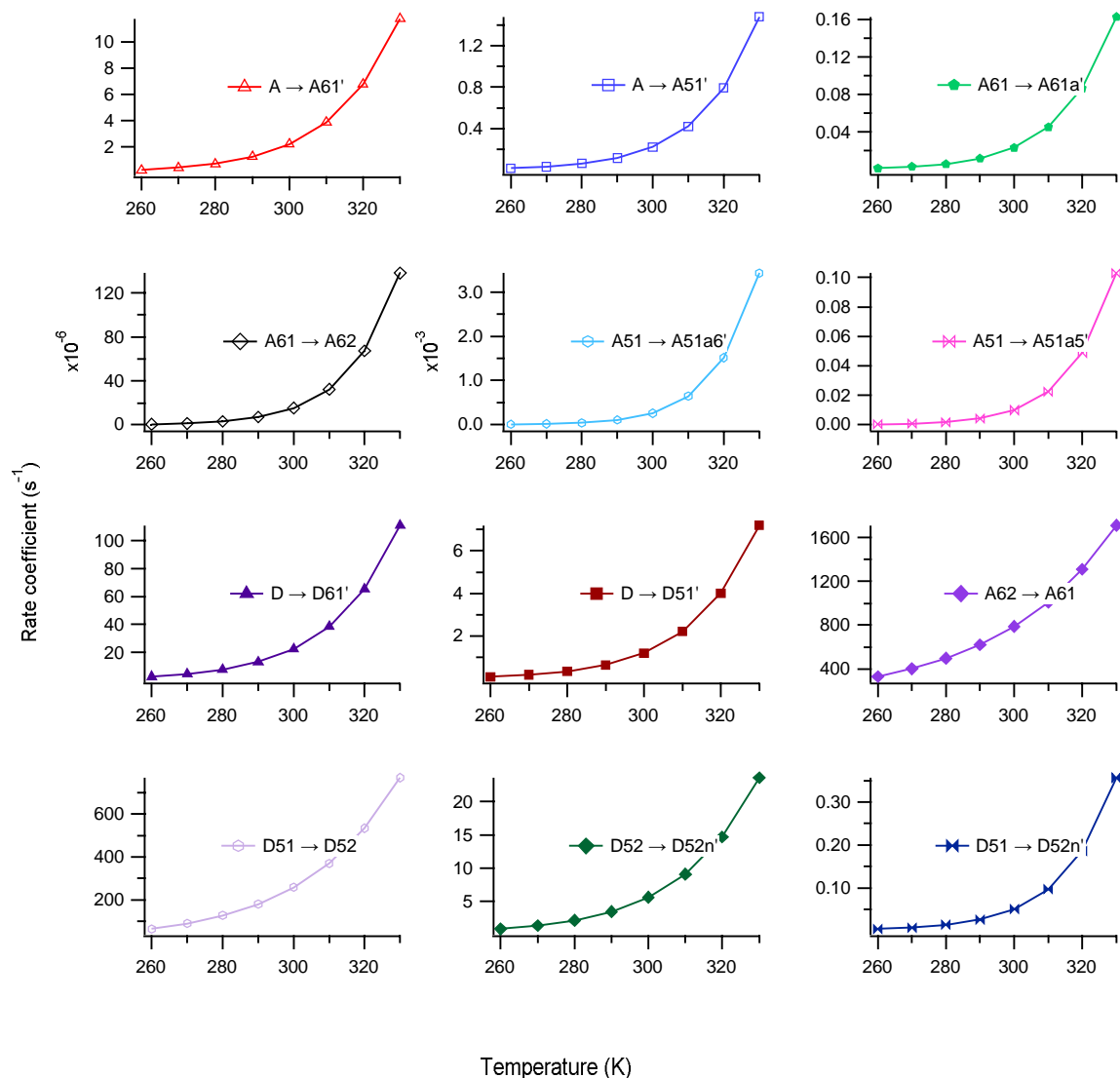
284 <sup>a</sup> below the product concentrations in the parenthesis are the reaction times.

285

## 286 S8: Temperature dependency of H-shift rate coefficients

287 In general, the H-shift reaction which are key to autoxidation are highly dependent on  
 288 temperature. To test this, we apply a temperature range of 260-330 K in the MESMER  
 289 simulation. Given that all our H-shift reactions have positive barriers, we observe a positive  
 290 temperature dependency in these reactions (see Supplementary Figure S9 and Table S5). The  
 291 results show that at 310 K, the H-shift rate coefficients are increased by factors of 1.3-3 relative  
 292 to the rate coefficients at 298.15 K. At 330 K, the factors increase to 2.3-8 for different H-shift  
 293 reactions. The second H-shift reactions which by a subsequent O<sub>2</sub> addition reaction lead to O<sub>7</sub>  
 294 HOM A61a' and D52n' (via C1 and C4 channels respectively) get faster by factors of 2.2 and  
 295 1.8 respectively at 310 K in terms of their rate coefficients. The factors for these H-shift  
 296 reactions increase to 8 and 4.6 respectively at a temperature of 330 K.





297

298 Figure S9: Positive temperature dependency of H-shift rate coefficients shown for the transition  
 299 of different intermediates (e.g., A→A61', A61→A62, etc.) along the path to HOM.

300

301 Supplementary Table S5: MESMER rate coefficients of H-shift reactions at different  
 302 simulation temperatures.

Transition	Rate coefficients (s-1) at different temperatures							
	260 K	270 K	280 K	290 K	300 K	310 K	320 K	330 K
A→A61'	2.34x10 <sup>-1</sup>	4.10x10 <sup>-1</sup>	7.20x10 <sup>-1</sup>	1.26	2.22	3.89	6.79	1.18x10 <sup>1</sup>
A→A51'	1.67x10 <sup>-2</sup>	3.19x10 <sup>-2</sup>	6.09x10 <sup>-2</sup>	1.16x10 <sup>-1</sup>	2.21x10 <sup>-1</sup>	4.20x10 <sup>-1</sup>	7.92x10 <sup>-1</sup>	1.48
A61→A61a'	1.29x10 <sup>-3</sup>	2.76x10 <sup>-3</sup>	5.75x10 <sup>-3</sup>	1.17x10 <sup>-2</sup>	2.32x10 <sup>-2</sup>	4.53x10 <sup>-2</sup>	8.68x10 <sup>-2</sup>	1.63x10 <sup>-1</sup>
A61→A62	5.82x10 <sup>-7</sup>	1.38x10 <sup>-6</sup>	3.17x10 <sup>-6</sup>	7.07x10 <sup>-6</sup>	1.53x10 <sup>-5</sup>	3.25x10 <sup>-5</sup>	6.75x10 <sup>-5</sup>	1.38x10 <sup>-4</sup>

A51→A51a6'	4.21X10 <sup>-6</sup>	1.29X10 <sup>-5</sup>	3.70X10 <sup>-5</sup>	1.01X10 <sup>-4</sup>	2.59X10 <sup>-4</sup>	6.39X10 <sup>-4</sup>	1.51X10 <sup>-3</sup>	3.43X10 <sup>-3</sup>
A51→A51a5'	2.65X10 <sup>-4</sup>	7.01X10 <sup>-4</sup>	1.77X10 <sup>-3</sup>	4.29X10 <sup>-3</sup>	9.99X10 <sup>-3</sup>	2.25X10 <sup>-2</sup>	4.89X10 <sup>-2</sup>	1.03X10 <sup>-1</sup>
D→D61'	2.62	4.50	7.70	1.32X10 <sup>1</sup>	2.26X10 <sup>1</sup>	3.85X10 <sup>1</sup>	6.54X10 <sup>1</sup>	1.11X10 <sup>2</sup>
D→D51'	9.15X10 <sup>-2</sup>	1.79X10 <sup>-1</sup>	3.44X10 <sup>-1</sup>	6.49X10 <sup>-1</sup>	1.21	2.21	4.01	7.19
A62→A61	3.30X10 <sup>2</sup>	4.03X10 <sup>2</sup>	4.97X10 <sup>2</sup>	6.22X10 <sup>2</sup>	7.88X10 <sup>2</sup>	1.01X10 <sup>3</sup>	1.31X10 <sup>3</sup>	1.71X10 <sup>3</sup>
D51→D52	6.44X10 <sup>1</sup>	9.02X10 <sup>1</sup>	1.27X10 <sup>2</sup>	1.81X10 <sup>2</sup>	2.58X10 <sup>2</sup>	3.70X10 <sup>2</sup>	5.33X10 <sup>2</sup>	7.69X10 <sup>2</sup>
D52→D52n'	8.56X10 <sup>-1</sup>	1.36	2.18	3.49	5.63	9.08	1.47X10 <sup>1</sup>	2.36X10 <sup>1</sup>
D51→D52n'	3.60X10 <sup>-3</sup>	6.93X10 <sup>-3</sup>	1.34X10 <sup>-2</sup>	2.59X10 <sup>-2</sup>	5.00X10 <sup>-2</sup>	9.66X10 <sup>-2</sup>	1.86X10 <sup>-1</sup>	3.57X10 <sup>-1</sup>

303

### 304 **S9: MESMER input for branching of D towards A62 and D51**

305 (Unimolecular H-shift reactions followed by pseudo-unimolecular O<sub>2</sub> addition reactions)

306 The example MESMER input contains all the geometries, vibrational frequencies, and

307 corrected relative energies of the studied species.

308

309 <?xml version="1.0" encoding="utf-8"?>

310 <?xml-stylesheet type='text/xsl' href='.././mesmer1.xsl'?>

311 <me:mesmer xmlns="http://www.xml-cml.org/schema"

312 xmlns:me="http://www.chem.leeds.ac.uk/mesmer"

313 xmlns:xsi="http://www.w3.org/2001/XMLSchema-instance">

314 <me:title>Unimolecular reactions of D</me:title>

315 <moleculeList>

316 <molecule id="C6H11O3-D" spinMultiplicity="2">

317 <atomArray>

318 <atom id="a1" elementType="C" hydrogenCount="1" x3="-2.707588" y3="-0.240514"

319 z3="-0.364066"/>

320 <atom id="a2" elementType="H" hydrogenCount="0" x3="-3.608384" y3="0.161997"

321 z3="-0.867971"/>

322 <atom id="a3" elementType="O" hydrogenCount="0" x3="-2.470574" y3="-1.418154"

323 z3="-0.398732"/>

324 <atom id="a4" elementType="C" hydrogenCount="2" x3="-1.868059" y3="0.786144"

325 z3="0.343080"/>

```
326 <atom id="a5" elementType="H" hydrogenCount="0" x3="-1.645911" y3="1.582943"
327 z3="-0.372793"/>
328 <atom id="a6" elementType="H" hydrogenCount="0" x3="-2.518628" y3="1.252841"
329 z3="1.089656"/>
330 <atom id="a7" elementType="C" hydrogenCount="2" x3="-0.604756" y3="0.243308"
331 z3="0.993245"/>
332 <atom id="a8" elementType="H" hydrogenCount="0" x3="-0.854162" y3="-0.627181"
333 z3="1.600523"/>
334 <atom id="a9" elementType="H" hydrogenCount="0" x3="-0.180523" y3="0.997016"
335 z3="1.656558"/>
336 <atom id="a10" elementType="C" hydrogenCount="1" x3="0.468040" y3="-0.184789"
337 z3="0.005911"/>
338 <atom id="a11" elementType="H" hydrogenCount="0" x3="0.061558" y3="-0.884551"
339 z3="-0.724064"/>
340 <atom id="a12" elementType="C" hydrogenCount="2" x3="1.699549" y3="-0.768724"
341 z3="0.672808"/>
342 <atom id="a13" elementType="H" hydrogenCount="0" x3="1.360710" y3="-1.600315"
343 z3="1.293524"/>
344 <atom id="a14" elementType="H" hydrogenCount="0" x3="2.116167" y3="-0.018070"
345 z3="1.346698"/>
346 <atom id="a15" elementType="C" hydrogenCount="3" x3="2.757726" y3="-1.250688"
347 z3="-0.310247"/>
348 <atom id="a16" elementType="H" hydrogenCount="0" x3="2.352979" y3="-2.009694"
349 z3="-0.981292"/>
350 <atom id="a17" elementType="H" hydrogenCount="0" x3="3.602403" y3="-1.688787"
351 z3="0.219709"/>
352 <atom id="a18" elementType="H" hydrogenCount="0" x3="3.134094" y3="-0.429746"
353 z3="-0.919232"/>
354 <atom id="a19" elementType="O" hydrogenCount="0" x3="0.840050" y3="0.948129"
355 z3="-0.849279"/>
356 <atom id="a20" elementType="O" hydrogenCount="0" x3="1.344302" y3="1.939415"
357 z3="-0.175202"/>
358 </atomArray>
359 <bondArray>
360 <bond atomRefs2="a16 a15" order="1"/>
361 <bond atomRefs2="a18 a15" order="1"/>
```

```
362 <bond atomRefs2="a2 a1" order="1"/>
363 <bond atomRefs2="a19 a20" order="1"/>
364 <bond atomRefs2="a19 a10" order="1"/>
365 <bond atomRefs2="a11 a10" order="1"/>
366 <bond atomRefs2="a3 a1" order="2"/>
367 <bond atomRefs2="a5 a4" order="1"/>
368 <bond atomRefs2="a1 a4" order="1"/>
369 <bond atomRefs2="a15 a17" order="1"/>
370 <bond atomRefs2="a15 a12" order="1"/>
371 <bond atomRefs2="a10 a12" order="1"/>
372 <bond atomRefs2="a10 a7" order="1"/>
373 <bond atomRefs2="a4 a7" order="1"/>
374 <bond atomRefs2="a4 a6" order="1"/>
375 <bond atomRefs2="a12 a13" order="1"/>
376 <bond atomRefs2="a12 a14" order="1"/>
377 <bond atomRefs2="a7 a8" order="1"/>
378 <bond atomRefs2="a7 a9" order="1"/>
379 </bondArray>
380 <propertyList>
381 <property dictRef="me:ZPE">
382 <scalar units="kcal/mol">0.0</scalar>
383 </property>
384 <property dictRef="me:rotConsts">
385 <array units="cm-1">0.082 0.033 0.027</array>
386 </property>
387 <property dictRef="me:symmetryNumber">
388 <scalar>1</scalar>
389 </property>
390 <property dictRef="me:vibFreqs">
391 <array units="cm-1">
```

```

392         440.60 73.15 93.23 134.47 138.80 200.70 220.01 245.83 310.61 320.21 398.72
393 485.44 593.66 667.65 725.42 780.58 821.11 871.50 939.58 949.90 995.34 1055.29 1068.61
394 1125.72 1137.97 1163.79 1220.81 1245.96 1270.27 1322.76 1332.17 1383.56 1397.28
395 1411.41 1420.92 1426.98 1429.49 1453.80 1471.02 1486.75 1506.65 1511.84 1838.30
396 2914.42 3046.12 3053.62 3061.54 3074.92 3084.32 3098.48 3112.41 3126.28 3131.10
397 3136.97
398     </array>
399 </property>
400 <property dictRef="me:MW">
401     <scalar>131.15</scalar>
402 </property>
403 <property dictRef="me:epsilon">
404     <scalar>343.0</scalar>
405 </property>
406 <property dictRef="me:sigma">
407     <scalar>6.25</scalar>
408 </property>
409 <property dictRef="me:spinMultiplicity">
410     <scalar>2</scalar>
411 </property>
412 </propertyList>
413 <me:energyTransferModel xsi:type="me:ExponentialDown">
414     <me:deltaEDown units="cm-1">225.0</me:deltaEDown>
415 </me:energyTransferModel>
416 </molecule>
417
418 <molecule id="D_1-6-aldHshift-TS">
419     <atomArray>
420     <atom id="a1" elementType="C" hydrogenCount="0" x3="2.171388" y3="0.048934" z3="-
421 0.247665"/>
422     <atom id="a2" elementType="O" hydrogenCount="0" x3="3.287959" y3="0.088910" z3="-
423 0.627350"/>

```

424 <atom id="a3" elementType="C" hydrogenCount="2" x3="1.255292" y3="-1.160226"  
425 z3="-0.175406"/>  
426 <atom id="a4" elementType="H" hydrogenCount="0" x3="0.783889" y3="-1.241738"  
427 z3="-1.157544"/>  
428 <atom id="a5" elementType="H" hydrogenCount="0" x3="1.884981" y3="-2.039904"  
429 z3="-0.040988"/>  
430 <atom id="a6" elementType="C" hydrogenCount="2" x3="0.214830" y3="-1.022117"  
431 z3="0.936377"/>  
432 <atom id="a7" elementType="H" hydrogenCount="0" x3="0.708013" y3="-0.665626"  
433 z3="1.840369"/>  
434 <atom id="a8" elementType="H" hydrogenCount="0" x3="-0.192406" y3="-2.005209"  
435 z3="1.173172"/>  
436 <atom id="a9" elementType="C" hydrogenCount="1" x3="-0.947718" y3="-0.084169"  
437 z3="0.587824"/>  
438 <atom id="a10" elementType="H" hydrogenCount="0" x3="-1.398134" y3="0.286239"  
439 z3="1.513740"/>  
440 <atom id="a11" elementType="C" hydrogenCount="2" x3="-2.017656" y3="-0.741095"  
441 z3="-0.271303"/>  
442 <atom id="a12" elementType="H" hydrogenCount="0" x3="-2.365067" y3="-1.627128"  
443 z3="0.263552"/>  
444 <atom id="a13" elementType="H" hydrogenCount="0" x3="-1.565969" y3="-1.092450"  
445 z3="-1.202612"/>  
446 <atom id="a14" elementType="C" hydrogenCount="3" x3="-3.197340" y3="0.172959"  
447 z3="-0.577401"/>  
448 <atom id="a15" elementType="H" hydrogenCount="0" x3="-3.661687" y3="0.527370"  
449 z3="0.344152"/>  
450 <atom id="a16" elementType="H" hydrogenCount="0" x3="-3.955731" y3="-0.356938"  
451 z3="-1.152644"/>  
452 <atom id="a17" elementType="H" hydrogenCount="0" x3="-2.882706" y3="1.044036"  
453 z3="-1.148722"/>  
454 <atom id="a18" elementType="O" hydrogenCount="0" x3="-0.491500" y3="1.041580"  
455 z3="-0.166657"/>  
456 <atom id="a19" elementType="O" hydrogenCount="1" x3="0.485120" y3="1.720209"  
457 z3="0.528334"/>  
458 <atom id="a20" elementType="H" hydrogenCount="0" x3="1.519405" y3="1.080043"  
459 z3="0.178357"/>  
460 </atomArray>

```
461 <bondArray>
462   <bond atomRefs2="a13 a11" order="1"/>
463   <bond atomRefs2="a4 a3" order="1"/>
464   <bond atomRefs2="a16 a14" order="1"/>
465   <bond atomRefs2="a17 a14" order="1"/>
466   <bond atomRefs2="a2 a1" order="2"/>
467   <bond atomRefs2="a14 a11" order="1"/>
468   <bond atomRefs2="a14 a15" order="1"/>
469   <bond atomRefs2="a11 a12" order="1"/>
470   <bond atomRefs2="a11 a9" order="1"/>
471   <bond atomRefs2="a1 a3" order="1"/>
472   <bond atomRefs2="a3 a5" order="1"/>
473   <bond atomRefs2="a3 a6" order="1"/>
474   <bond atomRefs2="a18 a19" order="1"/>
475   <bond atomRefs2="a18 a9" order="1"/>
476   <bond atomRefs2="a20 a19" order="1"/>
477   <bond atomRefs2="a9 a6" order="1"/>
478   <bond atomRefs2="a9 a10" order="1"/>
479   <bond atomRefs2="a6 a8" order="1"/>
480   <bond atomRefs2="a6 a7" order="1"/>
481 </bondArray>
482   <propertyList>
483     <property dictRef="me:ZPE">
484       <scalar units="kcal/mol">18.67</scalar>
485     </property>
486     <property dictRef="me:rotConsts">
487       <array units="cm-1">
488         0.104 0.031 0.028
489       </array>
490     </property>
```

```

491     <property dictRef="me:symmetryNumber">
492         <scalar>1</scalar>
493     </property>
494     <property dictRef="me:vibFreqs">
495         <array units="cm-1">
496             47.77 97.38 129.80 207.11 228.21 263.19 292.95 338.32 386.36 390.63 452.66
497             510.86 597.23 609.74 766.99 827.35 848.41 874.73 951.05 978.22 1017.83 1061.22 1080.44
498             1088.88 1097.35 1155.81 1183.00 1228.56 1256.97 1305.59 1332.93 1349.51 1371.85
499             1396.76 1419.91 1425.35 1447.49 1485.23 1500.47 1503.50 1513.27 1607.94 1925.47
500             3039.22 3050.59 3054.34 3065.86 3077.43 3092.19 3118.14 3120.90 3124.09 3144.45
501         </array>
502     </property>
503     <property dictRef="me:MW">
504         <scalar>131.15</scalar>
505     </property>
506     <property dictRef="me:imFreqs">
507         <scalar units="cm-1">1805.75</scalar>
508     </property>
509     <property dictRef="me:spinMultiplicity">
510         <scalar>2</scalar>
511     </property>
512 </propertyList>
513 <me:DOSCMMethod xsi:type="ClassicalRotors"/>
514 </molecule>
515
516 <molecule id="D61_pr">
517     <atomArray>
518         <atom id="a1" elementType="C" hydrogenCount="0" x3="-2.591004" y3="-0.009787"
519         z3="-0.357272"/>
520         <atom id="a2" elementType="O" hydrogenCount="0" x3="-2.535322" y3="0.972415"
521         z3="0.292868"/>
522         <atom id="a3" elementType="C" hydrogenCount="2" x3="-1.765467" y3="-1.268641"
523         z3="-0.278670"/>

```



524 <atom id="a4" elementType="H" hydrogenCount="0" x3="-2.448039" y3="-1.998674"  
525 z3="0.165560"/>  
526 <atom id="a5" elementType="H" hydrogenCount="0" x3="-1.591793" y3="-1.610412"  
527 z3="-1.299722"/>  
528 <atom id="a6" elementType="C" hydrogenCount="2" x3="-0.465352" y3="-1.171123"  
529 z3="0.520995"/>  
530 <atom id="a7" elementType="H" hydrogenCount="0" x3="-0.157903" y3="-2.179492"  
531 z3="0.802600"/>  
532 <atom id="a8" elementType="H" hydrogenCount="0" x3="-0.633886" y3="-0.622273"  
533 z3="1.448795"/>  
534 <atom id="a9" elementType="C" hydrogenCount="1" x3="0.679564" y3="-0.528312"  
535 z3="-0.255168"/>  
536 <atom id="a10" elementType="H" hydrogenCount="0" x3="0.818642" y3="-1.070521"  
537 z3="-1.197097"/>  
538 <atom id="a11" elementType="C" hydrogenCount="2" x3="1.989311" y3="-0.538171"  
539 z3="0.521288"/>  
540 <atom id="a12" elementType="H" hydrogenCount="0" x3="2.217204" y3="-1.577451"  
541 z3="0.770015"/>  
542 <atom id="a13" elementType="H" hydrogenCount="0" x3="1.842062" y3="-0.011980"  
543 z3="1.465088"/>  
544 <atom id="a14" elementType="C" hydrogenCount="3" x3="3.146410" y3="0.081218"  
545 z3="-0.249032"/>  
546 <atom id="a15" elementType="H" hydrogenCount="0" x3="3.312520" y3="-0.437604"  
547 z3="-1.194910"/>  
548 <atom id="a16" elementType="H" hydrogenCount="0" x3="4.068149" y3="0.026669"  
549 z3="0.329198"/>  
550 <atom id="a17" elementType="H" hydrogenCount="0" x3="2.945867" y3="1.127456"  
551 z3="-0.472606"/>  
552 <atom id="a18" elementType="O" hydrogenCount="0" x3="0.335468" y3="0.765424"  
553 z3="-0.740110"/>  
554 <atom id="a19" elementType="O" hydrogenCount="1" x3="0.247042" y3="1.667694"  
555 z3="0.357754"/>  
556 <atom id="a20" elementType="H" hydrogenCount="0" x3="-0.711102" y3="1.718909"  
557 z3="0.486140"/>  
558 </atomArray>  
559 <bondArray>

```
560 <bond atomRefs2="a5 a3" order="1"/>
561 <bond atomRefs2="a10 a9" order="1"/>
562 <bond atomRefs2="a15 a14" order="1"/>
563 <bond atomRefs2="a18 a9" order="1"/>
564 <bond atomRefs2="a18 a19" order="1"/>
565 <bond atomRefs2="a17 a14" order="1"/>
566 <bond atomRefs2="a1 a3" order="1"/>
567 <bond atomRefs2="a1 a2" order="2"/>
568 <bond atomRefs2="a3 a4" order="1"/>
569 <bond atomRefs2="a3 a6" order="1"/>
570 <bond atomRefs2="a9 a6" order="1"/>
571 <bond atomRefs2="a9 a11" order="1"/>
572 <bond atomRefs2="a14 a16" order="1"/>
573 <bond atomRefs2="a14 a11" order="1"/>
574 <bond atomRefs2="a19 a20" order="1"/>
575 <bond atomRefs2="a6 a7" order="1"/>
576 <bond atomRefs2="a6 a8" order="1"/>
577 <bond atomRefs2="a11 a12" order="1"/>
578 <bond atomRefs2="a11 a13" order="1"/>
579 </bondArray>
580 <propertyList>
581 <property dictRef="me:ZPE">
582 <scalar units="kcal/mol">2.87</scalar>
583 </property>
584 <property dictRef="me:rotConsts">
585 <array units="cm-1">
586 0.102 0.035 0.029
587 </array>
588 </property>
589 <property dictRef="me:symmetryNumber">
```

```

590     <scalar>1</scalar>
591 </property>
592 <property dictRef="me:vibFreqs">
593     <array units="cm-1">
594         67.19 82.78 121.62 150.00 182.52 189.81 207.85 265.10 304.05 321.73 401.49
595     482.85 522.10 582.51 647.59 764.50 795.32 840.28 874.94 936.86 960.32 1016.85 1024.01
596     1064.20 1097.54 1138.90 1150.35 1226.58 1243.76 1306.59 1316.70 1348.76 1377.98
597     1397.48 1409.89 1425.80 1444.43 1457.39 1479.98 1490.94 1503.94 1511.67 1941.48
598     3035.93 3050.65 3054.16 3059.27 3069.35 3099.99 3106.20 3116.03 3122.78 3142.14
599     3723.51
600 </array>
601 </property>
602 <property dictRef="me:MW">
603     <scalar>131.15</scalar>
604 </property>
605 <property dictRef="me:epsilon">
606     <scalar>343.0</scalar>
607 </property>
608 <property dictRef="me:sigma">
609     <scalar>6.25</scalar>
610 </property>
611 <property dictRef="me:spinMultiplicity">
612     <scalar>2</scalar>
613 </property>
614 </propertyList>
615 <me:energyTransferModel xsi:type="me:ExponentialDown">
616     <me:deltaEDown units="cm-1">225.0</me:deltaEDown>
617 </me:energyTransferModel>
618 </molecule>
619
620 <molecule id="C6H11O5-A62">
621     <atomArray>

```

622 <atom id="a1" elementType="H" hydrogenCount="0" x3="-3.299530" y3="-0.442021"  
623 z3="-1.556808"/>  
624 <atom id="a2" elementType="C" hydrogenCount="3" x3="-3.373600" y3="-1.102928"  
625 z3="-0.695105"/>  
626 <atom id="a3" elementType="H" hydrogenCount="0" x3="-4.133145" y3="-0.698268"  
627 z3="-0.024688"/>  
628 <atom id="a4" elementType="H" hydrogenCount="0" x3="-3.716512" y3="-2.077519"  
629 z3="-1.040749"/>  
630 <atom id="a5" elementType="C" hydrogenCount="2" x3="-2.030843" y3="-1.220494"  
631 z3="0.014110"/>  
632 <atom id="a6" elementType="H" hydrogenCount="0" x3="-1.300866" y3="-1.674410"  
633 z3="-0.659900"/>  
634 <atom id="a7" elementType="H" hydrogenCount="0" x3="-2.118514" y3="-1.884179"  
635 z3="0.876947"/>  
636 <atom id="a8" elementType="C" hydrogenCount="1" x3="-1.497534" y3="0.120203"  
637 z3="0.504450"/>  
638 <atom id="a9" elementType="H" hydrogenCount="0" x3="-2.301087" y3="0.661709"  
639 z3="1.012412"/>  
640 <atom id="a10" elementType="C" hydrogenCount="2" x3="-0.316526" y3="0.009499"  
641 z3="1.471109"/>  
642 <atom id="a11" elementType="H" hydrogenCount="0" x3="-0.643120" y3="-0.579497"  
643 z3="2.328861"/>  
644 <atom id="a12" elementType="H" hydrogenCount="0" x3="-0.070561" y3="1.001090"  
645 z3="1.850716"/>  
646 <atom id="a13" elementType="C" hydrogenCount="2" x3="0.929836" y3="-0.644360"  
647 z3="0.882652"/>  
648 <atom id="a14" elementType="H" hydrogenCount="0" x3="0.697788" y3="-1.521864"  
649 z3="0.282847"/>  
650 <atom id="a15" elementType="H" hydrogenCount="0" x3="1.585464" y3="-1.012316"  
651 z3="1.675832"/>  
652 <atom id="a16" elementType="C" hydrogenCount="0" x3="1.764972" y3="0.290348"  
653 z3="0.067524"/>  
654 <atom id="a17" elementType="O" hydrogenCount="0" x3="1.705666" y3="1.473157"  
655 z3="-0.019954"/>  
656 <atom id="a18" elementType="O" hydrogenCount="0" x3="-1.156013" y3="0.839719"  
657 z3="-0.671506"/>

```
658 <atom id="a19" elementType="O" hydrogenCount="1" x3="-1.021099" y3="2.215035"  
659 z3="-0.342899"/>  
660 <atom id="a20" elementType="H" hydrogenCount="0" x3="-0.060584" y3="2.294490"  
661 z3="-0.244798"/>  
662 <atom id="a21" elementType="O" hydrogenCount="0" x3="2.830727" y3="-0.291473"  
663 z3="-0.675756"/>  
664 <atom id="a22" elementType="O" hydrogenCount="0" x3="2.953572" y3="-1.584040"  
665 z3="-0.536024"/>  
666 </atomArray>  
667 <bondArray>  
668 <bond atomRefs2="a1 a2" order="1"/>  
669 <bond atomRefs2="a4 a2" order="1"/>  
670 <bond atomRefs2="a2 a3" order="1"/>  
671 <bond atomRefs2="a2 a5" order="1"/>  
672 <bond atomRefs2="a21 a22" order="1"/>  
673 <bond atomRefs2="a21 a16" order="1"/>  
674 <bond atomRefs2="a18 a19" order="1"/>  
675 <bond atomRefs2="a18 a8" order="1"/>  
676 <bond atomRefs2="a6 a5" order="1"/>  
677 <bond atomRefs2="a19 a20" order="1"/>  
678 <bond atomRefs2="a17 a16" order="2"/>  
679 <bond atomRefs2="a5 a8" order="1"/>  
680 <bond atomRefs2="a5 a7" order="1"/>  
681 <bond atomRefs2="a16 a13" order="1"/>  
682 <bond atomRefs2="a14 a13" order="1"/>  
683 <bond atomRefs2="a8 a9" order="1"/>  
684 <bond atomRefs2="a8 a10" order="1"/>  
685 <bond atomRefs2="a13 a10" order="1"/>  
686 <bond atomRefs2="a13 a15" order="1"/>  
687 <bond atomRefs2="a10 a12" order="1"/>  
688 <bond atomRefs2="a10 a11" order="1"/>  
689 </bondArray>
```

```

690     <propertyList>
691         <property dictRef="me:ZPE">
692             <scalar units="kcal/mol">-30.87</scalar>
693         </property>
694         <property dictRef="me:rotConsts">
695             <array units="cm-1">
696                 0.055 0.022 0.019
697             </array>
698         </property>
699         <property dictRef="me:symmetryNumber">
700             <scalar>1</scalar>
701         </property>
702         <property dictRef="me:vibFreqs">
703             <array units="cm-1">
704                 34.92 52.51 80.17 119.38 160.41 162.94 197.91 214.93 236.09 284.59 323.91 340.88
705                 414.11 496.53 511.37 517.24 569.86 599.10 643.02 765.57 770.38 870.19 903.98 938.47
706                 986.09 1011.86 1039.09 1063.16 1076.55 1090.81 1143.06 1190.91 1232.95 1247.85
707                 1267.81 1312.73 1337.83 1375.52 1392.80 1405.25 1423.88 1424.48 1452.48 1465.56
708                 1485.75 1494.79 1505.18 1513.85 1897.98 3042.61 3052.68 3054.11 3070.71 3080.88
709                 3091.96 3119.83 3124.56 3138.43 3143.35 3708.15
710             </array>
711         </property>
712         <property dictRef="me:MW">
713             <scalar>163.15</scalar>
714         </property>
715         <property dictRef="me:spinMultiplicity">
716             <scalar>2</scalar>
717         </property>
718     </propertyList>
719     <me:DOSCMMethod xsi:type="ClassicalRotors"/>
720 </molecule>
721

```

```
722 <molecule id="D_1-5Hshift_RR-TS">
723   <atomArray>
724     <atom id="a1" elementType="C" hydrogenCount="1" x3="-2.629360" y3="-0.283299"
725     z3="-0.224138"/>
726     <atom id="a2" elementType="H" hydrogenCount="0" x3="-3.605403" y3="0.232118"
727     z3="-0.279199"/>
728     <atom id="a3" elementType="O" hydrogenCount="0" x3="-2.379290" y3="-1.206994"
729     z3="-0.964757"/>
730     <atom id="a4" elementType="C" hydrogenCount="1" x3="-1.679910" y3="0.255775"
731     z3="0.756364"/>
732     <atom id="a5" elementType="C" hydrogenCount="2" x3="-0.426800" y3="-0.518010"
733     z3="1.029928"/>
734     <atom id="a6" elementType="H" hydrogenCount="0" x3="-0.612316" y3="-1.586320"
735     z3="0.903206"/>
736     <atom id="a7" elementType="H" hydrogenCount="0" x3="-0.072637" y3="-0.335185"
737     z3="2.043298"/>
738     <atom id="a8" elementType="C" hydrogenCount="1" x3="0.710774" y3="-0.147623"
739     z3="0.043884"/>
740     <atom id="a9" elementType="H" hydrogenCount="0" x3="0.415466" y3="-0.440234"
741     z3="-0.966317"/>
742     <atom id="a10" elementType="C" hydrogenCount="2" x3="2.048733" y3="-0.743659"
743     z3="0.428315"/>
744     <atom id="a11" elementType="H" hydrogenCount="0" x3="1.899804" y3="-1.816392"
745     z3="0.563595"/>
746     <atom id="a12" elementType="H" hydrogenCount="0" x3="2.342624" y3="-0.342239"
747     z3="1.401001"/>
748     <atom id="a13" elementType="C" hydrogenCount="3" x3="3.139806" y3="-0.491322"
749     z3="-0.604064"/>
750     <atom id="a14" elementType="H" hydrogenCount="0" x3="2.865342" y3="-0.913407"
751     z3="-1.571581"/>
752     <atom id="a15" elementType="H" hydrogenCount="0" x3="4.078143" y3="-0.948501"
753     z3="-0.292792"/>
754     <atom id="a16" elementType="H" hydrogenCount="0" x3="3.311413" y3="0.575487"
755     z3="-0.739574"/>
756     <atom id="a17" elementType="O" hydrogenCount="0" x3="0.839784" y3="1.267191"
757     z3="0.080579"/>
```

```
758 <atom id="a18" elementType="O" hydrogenCount="1" x3="-0.251036" y3="1.824014"  
759 z3="-0.523727"/>  
760 <atom id="a19" elementType="H" hydrogenCount="0" x3="-2.130636" y3="0.798245"  
761 z3="1.581944"/>  
762 <atom id="a20" elementType="H" hydrogenCount="0" x3="-1.146920" y3="1.271563"  
763 z3="0.037928"/>  
764 </atomArray>  
765 <bondArray>  
766 <bond atomRefs2="a14 a13" order="1"/>  
767 <bond atomRefs2="a9 a8" order="1"/>  
768 <bond atomRefs2="a3 a1" order="2"/>  
769 <bond atomRefs2="a16 a13" order="1"/>  
770 <bond atomRefs2="a13 a15" order="1"/>  
771 <bond atomRefs2="a13 a10" order="1"/>  
772 <bond atomRefs2="a18 a20" order="1"/>  
773 <bond atomRefs2="a18 a17" order="1"/>  
774 <bond atomRefs2="a2 a1" order="1"/>  
775 <bond atomRefs2="a1 a4" order="1"/>  
776 <bond atomRefs2="a8 a17" order="1"/>  
777 <bond atomRefs2="a8 a10" order="1"/>  
778 <bond atomRefs2="a8 a5" order="1"/>  
779 <bond atomRefs2="a10 a11" order="1"/>  
780 <bond atomRefs2="a10 a12" order="1"/>  
781 <bond atomRefs2="a4 a5" order="1"/>  
782 <bond atomRefs2="a4 a19" order="1"/>  
783 <bond atomRefs2="a6 a5" order="1"/>  
784 <bond atomRefs2="a5 a7" order="1"/>  
785 </bondArray>  
786 <propertyList>  
787 <property dictRef="me:ZPE">  
788 <scalar units="kcal/mol">21.09</scalar>
```



```

789     </property>
790     <property dictRef="me:rotConsts">
791         <array units="cm-1">
792             0.090 0.032 0.029
793         </array>
794     </property>
795     <property dictRef="me:symmetryNumber">
796         <scalar>1</scalar>
797     </property>
798     <property dictRef="me:vibFreqs">
799         <array units="cm-1">
800             58.88 101.46 102.90 173.21 209.10 240.96 270.76 307.56 381.97 444.39 502.42
801             521.99 643.83 676.41 769.49 782.12 879.16 900.15 953.23 970.22 1005.16 1048.14 1082.02
802             1114.17 1117.14 1129.50 1161.18 1174.34 1236.98 1288.13 1317.10 1350.06 1366.73
803             1393.98 1415.39 1425.05 1425.95 1463.56 1486.74 1504.89 1512.57 1556.93 1764.84
804             2943.00 3054.68 3055.75 3063.63 3071.97 3097.64 3127.11 3129.13 3139.53 3157.90
805         </array>
806     </property>
807     <property dictRef="me:MW">
808         <scalar>131.15</scalar>
809     </property>
810         <property dictRef="me:imFreqs">
811             <scalar units="cm-1">1935.56</scalar>
812         </property>
813     <property dictRef="me:spinMultiplicity">
814         <scalar>2</scalar>
815     </property>
816 </propertyList>
817 <me:DOSCMMethod xsi:type="ClassicalRotors"/>
818 </molecule>
819
820     <molecule id="D51_pr">

```

821 <atomArray>  
822 <atom id="a1" elementType="C" hydrogenCount="1" x3="2.424466" y3="-0.404465"  
823 z3="-0.601898"/>  
824 <atom id="a2" elementType="H" hydrogenCount="0" x3="3.032948" y3="-0.770016"  
825 z3="-1.443473"/>  
826 <atom id="a3" elementType="O" hydrogenCount="0" x3="2.723837" y3="0.648707" z3="-  
827 0.043837"/>  
828 <atom id="a4" elementType="C" hydrogenCount="1" x3="1.300936" y3="-1.202309"  
829 z3="-0.232773"/>  
830 <atom id="a5" elementType="H" hydrogenCount="0" x3="1.058882" y3="-2.042782"  
831 z3="-0.871849"/>  
832 <atom id="a6" elementType="C" hydrogenCount="2" x3="0.477540" y3="-0.948298"  
833 z3="0.971107"/>  
834 <atom id="a7" elementType="H" hydrogenCount="0" x3="1.047613" y3="-0.370167"  
835 z3="1.698014"/>  
836 <atom id="a8" elementType="H" hydrogenCount="0" x3="0.226104" y3="-1.912137"  
837 z3="1.420528"/>  
838 <atom id="a9" elementType="C" hydrogenCount="1" x3="-0.863829" y3="-0.204765"  
839 z3="0.741736"/>  
840 <atom id="a10" elementType="H" hydrogenCount="0" x3="-1.452279" y3="-0.327984"  
841 z3="1.655178"/>  
842 <atom id="a11" elementType="C" hydrogenCount="2" x3="-1.662375" y3="-0.725877"  
843 z3="-0.444346"/>  
844 <atom id="a12" elementType="H" hydrogenCount="0" x3="-1.750810" y3="-1.810396"  
845 z3="-0.336367"/>  
846 <atom id="a13" elementType="H" hydrogenCount="0" x3="-1.096320" y3="-0.541996"  
847 z3="-1.358230"/>  
848 <atom id="a14" elementType="C" hydrogenCount="3" x3="-3.041888" y3="-0.092880"  
849 z3="-0.551505"/>  
850 <atom id="a15" elementType="H" hydrogenCount="0" x3="-3.633506" y3="-0.282963"  
851 z3="0.345800"/>  
852 <atom id="a16" elementType="H" hydrogenCount="0" x3="-3.587949" y3="-0.494979"  
853 z3="-1.404139"/>  
854 <atom id="a17" elementType="H" hydrogenCount="0" x3="-2.960558" y3="0.985542"  
855 z3="-0.676653"/>  
856 <atom id="a18" elementType="O" hydrogenCount="0" x3="-0.689331" y3="1.200034"  
857 z3="0.724140"/>

```
858 <atom id="a19" elementType="O" hydrogenCount="1" x3="0.012856" y3="1.579026"
859 z3="-0.453707"/>
860 <atom id="a20" elementType="H" hydrogenCount="0" x3="0.927872" y3="1.617310"
861 z3="-0.135504"/>
862 </atomArray>
863 <bondArray>
864 <bond atomRefs2="a2 a1" order="1"/>
865 <bond atomRefs2="a16 a14" order="1"/>
866 <bond atomRefs2="a13 a11" order="1"/>
867 <bond atomRefs2="a5 a4" order="1"/>
868 <bond atomRefs2="a17 a14" order="1"/>
869 <bond atomRefs2="a1 a4" order="1"/>
870 <bond atomRefs2="a1 a3" order="2"/>
871 <bond atomRefs2="a14 a11" order="1"/>
872 <bond atomRefs2="a14 a15" order="1"/>
873 <bond atomRefs2="a19 a20" order="1"/>
874 <bond atomRefs2="a19 a18" order="1"/>
875 <bond atomRefs2="a11 a12" order="1"/>
876 <bond atomRefs2="a11 a9" order="1"/>
877 <bond atomRefs2="a4 a6" order="1"/>
878 <bond atomRefs2="a18 a9" order="1"/>
879 <bond atomRefs2="a9 a6" order="1"/>
880 <bond atomRefs2="a9 a10" order="1"/>
881 <bond atomRefs2="a6 a8" order="1"/>
882 <bond atomRefs2="a6 a7" order="1"/>
883 </bondArray>
884 <propertyList>
885 <property dictRef="me:ZPE">
886 <scalar units="kcal/mol">6.16</scalar>
887 </property>
888 <property dictRef="me:rotConsts">
```

```

889     <array units="cm-1">
890         0.094 0.035 0.031
891     </array>
892 </property>
893 <property dictRef="me:symmetryNumber">
894     <scalar>1</scalar>
895 </property>
896 <property dictRef="me:vibFreqs">
897     <array units="cm-1">
898         56.02 81.32 120.30 168.43 177.90 201.16 256.70 263.21 301.84 348.54 406.83
899     518.23 589.73 614.76 706.07 722.14 777.39 811.74 908.59 943.33 981.47 1003.45 1017.61
900     1025.87 1083.52 1123.74 1156.18 1176.74 1264.20 1269.39 1316.43 1342.24 1385.29
901     1405.96 1415.93 1424.32 1455.33 1467.30 1485.70 1486.75 1503.83 1510.97 1634.96
902     2987.94 3047.56 3049.89 3051.31 3064.22 3100.07 3119.44 3123.22 3141.40 3189.68
903     3705.66
904     </array>
905 </property>
906 <property dictRef="me:MW">
907     <scalar>131.15</scalar>
908 </property>
909 <property dictRef="me:epsilon">
910     <scalar>343.0</scalar>
911 </property>
912 <property dictRef="me:sigma">
913     <scalar>6.25</scalar>
914 </property>
915 <property dictRef="me:spinMultiplicity">
916     <scalar>2</scalar>
917 </property>
918 </propertyList>
919 <me:energyTransferModel xsi:type="me:ExponentialDown">
920     <me:deltaEDown units="cm-1">225.0</me:deltaEDown>

```

```
921     </me:energyTransferModel>
922 </molecule>
923
924     <molecule id="C6H11O5-D51">
925     <atomArray>
926     <atom id="a1" elementType="C" hydrogenCount="1" x3="-1.679583" y3="1.016706"
927     z3="-0.232156"/>
928     <atom id="a2" elementType="H" hydrogenCount="0" x3="-2.025198" y3="0.878997"
929     z3="-1.269083"/>
930     <atom id="a3" elementType="O" hydrogenCount="0" x3="-1.484024" y3="2.104712"
931     z3="0.242018"/>
932     <atom id="a4" elementType="C" hydrogenCount="1" x3="-1.509098" y3="-0.252399"
933     z3="0.588005"/>
934     <atom id="a5" elementType="H" hydrogenCount="0" x3="-2.231053" y3="-0.213646"
935     z3="1.405441"/>
936     <atom id="a6" elementType="C" hydrogenCount="2" x3="-0.099885" y3="-0.442493"
937     z3="1.120948"/>
938     <atom id="a7" elementType="H" hydrogenCount="0" x3="-0.067627" y3="-1.353504"
939     z3="1.718606"/>
940     <atom id="a8" elementType="H" hydrogenCount="0" x3="0.118056" y3="0.391478"
941     z3="1.789051"/>
942     <atom id="a9" elementType="C" hydrogenCount="1" x3="0.957465" y3="-0.511050"
943     z3="0.022390"/>
944     <atom id="a10" elementType="H" hydrogenCount="0" x3="0.707955" y3="-1.313333"
945     z3="-0.677086"/>
946     <atom id="a11" elementType="C" hydrogenCount="2" x3="2.354760" y3="-0.744185"
947     z3="0.575827"/>
948     <atom id="a12" elementType="H" hydrogenCount="0" x3="2.328387" y3="-1.675630"
949     z3="1.146132"/>
950     <atom id="a13" elementType="H" hydrogenCount="0" x3="2.592796" y3="0.052586"
951     z3="1.281407"/>
952     <atom id="a14" elementType="C" hydrogenCount="3" x3="3.420180" y3="-0.824068"
953     z3="-0.507815"/>
954     <atom id="a15" elementType="H" hydrogenCount="0" x3="3.200881" y3="-1.623803"
955     z3="-1.217151"/>
```

956 <atom id="a16" elementType="H" hydrogenCount="0" x3="4.398358" y3="-1.021967"  
957 z3="-0.071457"/>  
958 <atom id="a17" elementType="H" hydrogenCount="0" x3="3.478549" y3="0.110166"  
959 z3="-1.063457"/>  
960 <atom id="a18" elementType="O" hydrogenCount="0" x3="0.877714" y3="0.629090"  
961 z3="-0.832288"/>  
962 <atom id="a19" elementType="O" hydrogenCount="1" x3="1.318906" y3="1.780465"  
963 z3="-0.125327"/>  
964 <atom id="a20" elementType="H" hydrogenCount="0" x3="0.481012" y3="2.233918"  
965 z3="0.058295"/>  
966 <atom id="a21" elementType="O" hydrogenCount="0" x3="-1.840896" y3="-1.402382"  
967 z3="-0.219239"/>  
968 <atom id="a22" elementType="O" hydrogenCount="0" x3="-3.077343" y3="-1.351927"  
969 z3="-0.628151"/>  
970 </atomArray>  
971 <bondArray>  
972 <bond atomRefs2="a2 a1" order="1"/>  
973 <bond atomRefs2="a15 a14" order="1"/>  
974 <bond atomRefs2="a17 a14" order="1"/>  
975 <bond atomRefs2="a18 a19" order="1"/>  
976 <bond atomRefs2="a18 a9" order="1"/>  
977 <bond atomRefs2="a10 a9" order="1"/>  
978 <bond atomRefs2="a22 a21" order="1"/>  
979 <bond atomRefs2="a14 a16" order="1"/>  
980 <bond atomRefs2="a14 a11" order="1"/>  
981 <bond atomRefs2="a1 a3" order="2"/>  
982 <bond atomRefs2="a1 a4" order="1"/>  
983 <bond atomRefs2="a21 a4" order="1"/>  
984 <bond atomRefs2="a19 a20" order="1"/>  
985 <bond atomRefs2="a9 a11" order="1"/>  
986 <bond atomRefs2="a9 a6" order="1"/>  
987 <bond atomRefs2="a11 a12" order="1"/>  
988 <bond atomRefs2="a11 a13" order="1"/>

```

989 <bond atomRefs2="a4 a6" order="1"/>
990 <bond atomRefs2="a4 a5" order="1"/>
991 <bond atomRefs2="a6 a7" order="1"/>
992 <bond atomRefs2="a6 a8" order="1"/>
993 </bondArray>
994 <propertyList>
995 <property dictRef="me:ZPE">
996 <scalar units="kcal/mol">-13.59</scalar>
997 </property>
998 <property dictRef="me:rotConsts">
999 <array units="cm-1">
1000 0.056 0.025 0.020
1001 </array>
1002 </property>
1003 <property dictRef="me:symmetryNumber">
1004 <scalar>1</scalar>
1005 </property>
1006 <property dictRef="me:vibFreqs">
1007 <array units="cm-1">
1008 62.55 71.80 97.45 117.72 149.76 183.99 206.03 213.77 228.86 286.52 298.07 332.45
1009 357.21 422.38 480.16 503.17 577.88 597.43 655.76 786.83 826.75 870.19 910.67 954.64
1010 986.44 1016.35 1029.14 1045.27 1098.16 1123.53 1148.46 1185.06 1250.26 1263.50
1011 1290.83 1316.87 1325.16 1334.00 1380.94 1398.91 1412.29 1416.35 1427.34 1471.53
1012 1473.98 1488.40 1504.96 1511.77 1820.68 2996.38 3053.21 3058.27 3068.30 3079.98
1013 3091.84 3103.17 3125.57 3130.21 3142.82 3689.10
1014 </array>
1015 </property>
1016 <property dictRef="me:MW">
1017 <scalar>163.15</scalar>
1018 </property>
1019 <property dictRef="me:spinMultiplicity">
1020 <scalar>2</scalar>

```

```
1021     </property>
1022 </propertyList>
1023 <me:DOSCMMethod xsi:type="ClassicalRotors"/>
1024 </molecule>
1025
1026 <molecule id="O2">
1027   <atomArray>
1028     <atom id="a1" elementType="O" hydrogenCount="0" x3="0.000000" y3="0.000000"
1029     z3="0.597994"/>
1030     <atom id="a2" elementType="O" hydrogenCount="0" x3="0.000000" y3="0.000000" z3="-
1031     0.597994"/>
1032   </atomArray>
1033   <bondArray>
1034     <bond atomRefs2="a2 a1" order="2"/>
1035   </bondArray>
1036   <propertyList>
1037     <property dictRef="me:ZPE">
1038       <scalar units="kcal/mol">0.00</scalar>
1039     </property>
1040     <property dictRef="me:rotConsts">
1041       <array units="cm-1">
1042         1.473
1043       </array>
1044     </property>
1045     <property dictRef="me:symmetryNumber">
1046       <scalar>2</scalar>
1047     </property>
1048     <property dictRef="me:vibFreqs">
1049       <array units="cm-1">
1050         1703.81
1051       </array>
```



```

1052     </property>
1053     <property dictRef="me:MW">
1054         <scalar>32</scalar>
1055     </property>
1056     <property dictRef="me:spinMultiplicity">
1057         <scalar>3</scalar>
1058     </property>
1059 </propertyList>
1060 <me:DOSCMMethod xsi:type="ClassicalRotors"/>
1061 </molecule>
1062
1063 <molecule id="N2">
1064     <propertyList>
1065         <property dictRef="me:epsilon">
1066             <scalar>48.0</scalar>
1067         </property>
1068         <property dictRef="me:sigma">
1069             <scalar>3.9</scalar>
1070         </property>
1071         <property dictRef="me:MW">
1072             <scalar units="amu">28.0</scalar>
1073         </property>
1074     </propertyList>
1075 </molecule>
1076 </moleculeList>
1077
1078 <reactionList>
1079     <reaction id="R1">
1080         <reactant>
1081             <molecule ref="C6H11O3-D" role="modelled" />

```

```

1082     </reactant>
1083     <product>
1084         <molecule ref="D61_pr" role="modelled" />
1085     </product>
1086         <me:transitionState>
1087             <molecule ref="D_1-6-aldHshift-TS" role="transitionState" />
1088         </me:transitionState>
1089             <me:tunneling name="Eckart" />
1090         <me:MCRCMethod name="RRKM"/>
1091     </reaction>
1092         <reaction id="R2">
1093             <reactant>
1094                 <molecule ref="C6H11O3-D" role="modelled" />
1095             </reactant>
1096             <product>
1097                 <molecule ref="D51_pr" role="modelled" />
1098             </product>
1099                 <me:transitionState>
1100                     <molecule ref="D_1-5Hshift_RR-TS" role="transitionState" />
1101                 </me:transitionState>
1102                     <me:tunneling name="Eckart" />
1103                 <me:MCRCMethod name="RRKM"/>
1104             </reaction>
1105             <reaction id="R3">
1106                 <reactant>
1107                     <molecule ref="D61_pr" me:type="modelled"/>
1108                 </reactant>
1109                 <reactant>
1110                     <molecule ref="O2" me:type="excessReactant"/>
1111                 </reactant>

```

```

1112     <product>
1113         <molecule ref="C6H11O5-A62" me:type="sink"/>
1114     </product>
1115     <me:MCRCMethod name="SimpleBimolecularSink" />
1116     <me:BimolecularLossRateCoefficient>2E-12</me:BimolecularLossRateCoefficient>
1117     <me:excessReactantConc>5.0E18</me:excessReactantConc>
1118 </reaction>
1119     <reaction id="R4">
1120     <reactant>
1121         <molecule ref="D51_pr" me:type="modelled"/>
1122     </reactant>
1123     <reactant>
1124         <molecule ref="O2" me:type="excessReactant"/>
1125     </reactant>
1126     <product>
1127         <molecule ref="C6H11O5-D51" me:type="sink"/>
1128     </product>
1129     <me:MCRCMethod name="SimpleBimolecularSink" />
1130     <me:BimolecularLossRateCoefficient>2E-12</me:BimolecularLossRateCoefficient>
1131     <me:excessReactantConc>5.0E18</me:excessReactantConc>
1132 </reaction>
1133 </reactionList>
1134
1135 <!-- Data taken from Seakins et al, J. Phys. Chem. Vol. 97, p. 4450 (1993). -->
1136 <me:conditions>
1137     <me:bathGas>N2</me:bathGas>
1138     <me:PTs>
1139         <me:PTpair units="Torr" P="760.00" T="298.15" precision="qd" />
1140     </me:PTs>
1141 </me:conditions>

```

1142  
1143 <me:modelParameters>  
1144 <me:grainSize units="cm-1">100</me:grainSize>  
1145 <me:energyAboveTheTopHill>30</me:energyAboveTheTopHill>  
1146 </me:modelParameters>  
1147  
1148 <me:control>  
1149 <me:ForceMacroDetailedBalance/>  
1150 <me:testDOS />  
1151 <me:printSpeciesProfile />  
1152 <me:testMicroRates />  
1153 <me:testRateConstants />  
1154 <me:printGrainDOS />  
1155 <me:printTunnellingCoefficients />  
1156 <me:printGrainkfE />  
1157 <me:printGrainkbE />  
1158 <me:eigenvalues>3</me:eigenvalues>  
1159 </me:control>  
1160 </me:mesmer>

1161  
1162

## 1163 **References**

- 1164 [1] Jenkin, M. E.; Valorso, R.; Aumont, B.; Rickard, A. R.; Wallington, T. J. Estimation of  
1165 rate coefficients and branching ratios for gas-phase reactions of OH with aliphatic organic  
1166 compounds for use in automated mechanism construction. *Atmos. Chem. Phys.* **2018**, 18, 9297-  
1167 9328.
- 1168 [2] Ziemann, P. J.; Atkinson, R. Kinetics, products, and mechanisms of secondary organic  
1169 aerosol formation. *Chem. Soc. Rev.* **2012**, 41, 6582-6605.
- 1170 [3] Møller, K. H.; Otkjær, R. V.; Hyttinen, N.; Kurtén, T.; Kjaergaard, H. G. Cost-effective  
1171 implementation of multiconformer transition state theory for peroxy radical hydrogen shift  
1172 reactions. *The Journal of Physical Chemistry A* **2016**, 120, 10072–10087.

- 1173 [4] Castañeda, R.; Iuga, C.; Álvarez-Idaboy, J. R.; Vivier-Bunge, A. Rate constants and  
1174 branching ratios in the oxidation of aliphatic aldehydes by OH radicals under atmospheric  
1175 conditions. *Journal of the Mexican Chemical Society* **2012**, 56, 316–324.
- 1176 [5] Henriksen, N. E.; Hansen, F. Y. Theories of molecular reaction dynamics: the  
1177 microscopic foundation of chemical kinetics, *Oxford University Press* **2018**.
- 1178 [6] Bunker, D. L.; Garrett, B.; Kliendienst, T.; Long III, G. S. Discrete simulation methods in  
1179 combustion kinetics. *Combustion and Flame* **1974**, 23, 373-379.
- 1180 [7] Gillespie, D. T. A general method for numerically simulating the stochastic time evolution  
1181 of coupled chemical reactions. *J. Comput. Phys.* **1976**, 22, 403-434.
- 1182 [8] Williams, I. D.; Revitt, D. M.; Hamilton, R. S. A comparison of carbonyl compound  
1183 concentrations at urban roadside and indoor sites. *The Science of the Total Environment*  
1184 **1996**, 189/190, 475-483.
- 1185 [9] Ciccioli, P.; Brancaleoni, E.; Frattoni, M.; Cecinato, A.; Brachetti, A. Ubiquitous  
1186 occurrence of semi-volatile carbonyl compounds in tropospheric samples and their possible  
1187 sources. *Atmospheric Environment* **1993**, Vol. 27A, No. 12, pp. 1891–1901.
- 1188 [10] Berndt, T.; Scholz, W.; Mentler, B.; Fischer, L.; Herrmann, H.; Kulmala, M.; Hansel, A.  
1189 Accretion Product Formation from Self- and Cross-Reactions of RO<sub>2</sub> Radicals in the  
1190 Atmosphere. *Angew. Chem. Int. Ed.* **2018**, 57, 3820-3824.
- 1191 [11] Jenkin, M. E.; Valorso, R.; Aumont, B.; Rickard, A. R. Estimation of Rate Coefficients  
1192 and Branching Ratios for Reactions of Organic Peroxy Radicals for use in Automated  
1193 Mechanism Construction. *Atmos. Chem. Phys. Diss.* **2019**, [https://doi.org/10.5194/acp-2019-](https://doi.org/10.5194/acp-2019-44)  
1194 44.